PATENT APPLICATION

IN THE UNITED STATES PATENT AND TRADEMARK OFFICE

In re Patent Application

Brockhaus et al.

Group 1806
Examiner D. Adams

Serial No. 08/095,640, filed July 21, 1993

For: HUMAN TNF RECEPTOR

DECLARATION [II] OF DR. WERNER LESSLAUER UNDER 37 C.F.R. §1.132

Honorable Commissioner of Patents and Trademarks

Washington, D.C. 20231

S i r:

I, DR. WERNER LESSLAUER, a citizen and resident of Basle, Switzerland, declare as follows:

I am the declarant of the Declaration [I] filed together with this Declaration.

From 1987 until the present, I have been employed in the biology departments of the Central Research Unit and the Central Nervous System Research Department of F.Hoffmann-La Roche Ltd, Basel, Switzerland [Roche] where my present position is that of Scientific Expert, responsible for directing and leading various research groups in protein, cell and molecular biology.

Part of my duties at Roche has involved methods and procedures for protein purification and testing carried out with

such proteins which include the TNF-α receptor protein as well as fusion proteins containing the TNF-α receptor protein.

I am one of the co-inventors of the invention disclosed in the captioned application which claims a soluble TNF-α receptor/IgG fusion protein and I have been involved and familiar with the preparation and testing of said fusion protein.

As seen from Evans et al., Journal of Experimental Medicine, Rockefeller University Press, Vol. 180, December 1994, pp. 2173-2179 which is attached herein as Exhibit A, there are two distinct TNF-α receptor proteins, i.e., a 75 kDa protein and a 55 kDa protein which cell membrane receptor proteins have soluble or extracellular portions in addition to transmembrane and intracellular portions.

The captioned application claims a fusion protein formed by the fusion of the soluble or extracellular portion of the TNF-α receptor and parts of the IgG heavy chains as well as claims those specific fusion proteins where the TNF-α receptor in the fusion protein constitutes the extracellular or soluble portion of either the 55 kDa protein or the 75 kDa protein.

This Declaration is submitted to demonstrate:

a) that the claimed TNF-α receptor IgG fusion protein [TNFR/IgG] has superior activity which cannot be

predicted from the activity of the TNF receptor protein itself or from the CD4/IgG fusion protein disclosed by Capon et al., Vol. 337, p. 525, February 9, 1984 in that:

1) the TNFR/IgG has far superior binding affinity for its ligand in relation to the binding affinity of the respective soluble receptor and

2) the TNFR/IgG has far superior activity in neutralizing TNF cytotoxicity than the soluble receptors themselves; and

b) that the claimed 55 kDa soluble TNF-α receptor/IgG fusion protein [55 TNFR/IgG] has far superior properties when compared to the 75 kDa soluble TNF-α receptor/IgG fusion protein [75 TNFR/IgG].

Fusion Protein Has Superior
Properties Over The Receptor Protein

To demonstrate that the soluble portion of 55 TNFR/IgG fusion protein has far superior properties than the soluble 55 TNF receptor protein, the following reference in addition to Evans of Exhibit A is attached and made Exhibit B:

Loetscher et al., Journal of Biological Chemistry, No. 27, pp. 18324, September 25, 1991 [Loetscher].

To demonstrate that the soluble portion of TNF receptor/fusion protein has superior properties which could not be predicted from the CD4/IgG fusion protein, the following reference is attached as Exhibit C:

Capon et al., Nature, Vol. 337, February 9, 1989, p. 525 [Capon].

I am one of the co-authors of the Loetscher article and the Evans article and am familiar and have participated in the preparation and testing of the soluble TNF-α receptors and its IgG fusion proteins as reported in these articles.

Loetscher and Evans [Exhibits A and B] disclose the recombinant soluble form of the human 55 TNF receptor protein, which has an apparent molecular weight of about 28 kDa as well as recombinant expression and purification from cell culture supernatants of the IgG fusion proteins formed with each of the soluble portion of the 75 TNF receptor being called TNFR-α and the soluble portion of the 55 kDa portion being called TNFR-ß.

Fig. 2 of Loetscher [Exhibit B] sets forth the dissociation constants [K_d] of the recombinant extracellular 55 TNFR protein and the 55 kDa TNFR/IgG fusion protein with TNF-α and TNF-ß ligands.

The dissociation constant, K_d represents the interaction of the receptor protein with its ligands, with the reciprocal of the K_d being the equilibrium constant.

The equilibrium constant represents the association of a receptor protein and its ligand. The greater the equilibrium constant the greater the amount of such binding which occurs under given conditions.

In view of the fact that the equilibrium constant is the reciprocal of the dissociation constant K_d, the lower the dissociation constant, the higher the equilibrium constant and the greater the affinity of the receptor to bind its ligand.

In Fig. 2 of Loetscher, the K_d values for the 55 TNFR/IgG fusion protein and the 55 TNFR protein with their ligands TNF-α and TNF-ß were determined by the Scatchard analysis which is the standard method for determining K_d.

As seen from the bottom six graphs in Fig. 2 of Loetscher, the results of the K_ds are as follows:

	K_d Ligand	
Protein	TNF-α	TNF-ß
55 TNFR (Baculovirus)	0.38 nM	0.52 nM
55 TNFR	0.34 nM	1.60 nM
55 TNFR/IgG	0.10 nM	0.12 nM

As seen from the results in this Table, the 55 TNFR/IgG fusion protein has at least a 3-fold smaller K_d, and therefore at least three times greater binding affinity than the corresponding soluble TNFR protein.

In Fig. 5 of Loetscher [Exhibit B], the dose-dependent inhibition of TNF cytotoxicity by the 55 TNFR/IgG fusion protein and the soluble 55 TNFR receptor protein is demonstrated utilizing the cytotoxic agents TNF-α [graph A] and TNF-ß [graph B].

As stated in Loetscher [Exhibit B], in reviewing the results of their test which demonstrates that the TNFR-ß/IgG fusion protein, referred to by Loetscher as rsTNFRß-hγ3, was markedly more effective than the soluble 55 TNF receptor protein, which Loetscher refers to as rsTNFRß (p. 18327):

> "As expected from the binding studies, rsTNFRß-hγ3 very efficiently inhibited TNF activity; at a concentration of 0.1 pmol/ml, i.e., equimolar to the TNFα concentration used in the assay, rsTNFRß-hγ3 prevented TNFα-induced cytolysis very efficiently (Fig. 5A). rsTNFRß also had inhibitory activity but a concentration about 100-fold in excess of TNFα was needed for complete inhibition. TNFß-induced cytotoxicity was also inhibited by the fusion protein, albeit not at equimolar concentrations. The protective effects of rsTNFRß in these cytotoxicity assays were only evident at rather high concentrations (Fig. 5ß)."

As shown in Fig. 5, the protection of cells from the cytotoxic activity of TNF-α and TNF-ß with the 55 TNF/IgG receptor fusion protein at a given dose level was much greater when

compared to the survival level of these cells protected by the extracellular domain of the 55 TNF receptor protein.

Fig. 5 in Capon compares the inhibition of infection of cells through the use of recombinant soluble CD4 [rCD4] to inhibition afforded by the CD4/IgG fusion proteins which Capon refers to as the CD4 immunoadhesins and Capon concludes in the statement on p. 529, right bottom of Exhibit C that

> "Both the CD4 immunoadhesins blocked cell killing with the same potency as soluble rCD4, without inhibiting cell proliferation..."

Furthermore, the dissociation constant K_d for the interaction of two distinct CD4/IgG molecules with their ligand gp 120 was indistinguishable from that of soluble CD4, demonstrating that the CD4/IgG fusion proteins exhibit no greater inhibition of infection from that obtained by the soluble CD4 protein and that the affinity of the soluble CD4 protein and the soluble CD4/IgG fusion protein for its ligands are the same.

Superior Properties of the 55 kDa Fusion Protein

Evans [Exhibit A] compares the ability of the 55 TNFR-IgG and 75 TNFR/IgG fusion proteins to protect against death in a murine model of gram negative sepsis with the results of this study with regard to the 75 fusion protein being set forth in Fig. 1 and 3 and the results with regard to the 55 fusion protein being set forth in Fig. 5 and 6.

In Fig. 1 and 3 of Evans, the dose of the 75 TNF/IgG protein given is 250 μg while the dose of the 55 TNF/IgG protein in Fig. 5 is far lower, i.e., 50 μg and in Fig. 6 is 200 μg per animal.

Comparing the results in Fig. 1 with those in Fig. 5 at 30 hours, approximately 60% of the mice treated with a 50 μg dose of 55 TNF/IgG survived whereas only about 40% of the mice treated with 75 TNFR/IgG survived even though a higher dose of 250 μg was utilized.

More importantly as seen by the results of Fig. 6 of Evans, when the dose of the 55 TNFR/IgG fusion protein is increased to 200 μg, 50 μg less than the dose of the 75 TNFR/IgG fusion protein in Fig. 1 and Fig. 3, over 80% survival was obtained after about 70 hours as compared to 30% (Fig. 1) or even 10% (Fig. 3) survival during this period with a higher dose of 75 TNFR/IgG (Fig. 1 and 3. of Evans).

Conclusion

1. As seen from the above results, the soluble 55 TNF-α receptor IgG fusion protein has superior binding activity to its ligands than that of the soluble 55 TNF-α receptor itself.

2. As seen from the above results, the soluble 55 TNFR/IgG

fusion protein has superior activity in neutralizing TNF cytotoxicity than the soluble receptor protein.

3. The ability of the soluble TNF-α receptor/IgG fusion protein to demonstrate superior binding activity to its ligand and superior neutralization of TNF cytotoxicity than the receptor protein itself makes this fusion protein a far superior pharmacological agent in combatting TNF challenges to the system than the soluble receptor protein from which the fusion protein is formed.

4. That the far superior pharmacological activity of the 55 TNF-α receptor/IgG fusion protein over the soluble 55 TNF-α receptor protein cannot be predicted from a comparable activity of IgG fusion proteins with other receptor proteins since as seen from the above results, the IgG fusion protein formed with the soluble portion of CD4 does not demonstrate such superior pharmacological activity when compared with the soluble CD4 protein itself.

5. That the foregoing results demonstrate that the 55 kDa soluble TNF-α receptor/IgG fusion protein has far greater pharmacological activity than the corresponding 75 kDa soluble TNF-α receptor IgG fusion protein in the animal model for gram negative sepsis.

I hereby declare that all statements made herein of my own

knowledge are true and that all statements made on information and belief are believed to be true; and further that these statements were made with the knowledge that willful false statements and the like so made are punishable by fine or imprisonment, or both, under Section 1001 of Title 18 of the United States Code and that such willful false statements may jeopardize the validity of the application or any patent issued thereon.

Date December 14, 1995

Werner Lesslauer

Werner Lesslauer

105671

Protective Effect of 55- but not 75-kD Soluble Tumor Necrosis Factor Receptor-Immunoglobulin G Fusion Proteins in an Animal Model of Gram-negative Sepsis

By T. J. Evans,* D. Moyes,* A. Carpenter,* R. Martin,* H. Loetscher,‡ W. Lesslauer,‡ and J. Cohen*

*From the *Department of Infectious Diseases and Bacteriology, Royal Postgraduate Medical School, London W12 0NN, UK; and ‡F. Hoffman-La Roche AG, CH4002 Basel, Switzerland*

Summary

The aim of this study was to compare the ability of both a 55- and 75-kD soluble tumor necrosis factor receptor immunoglobulin G fusion protein (sTNFR-IgG) in protecting against death in a murine model of gram-negative sepsis. Pretreatment with 250 μg of the p75 construct delayed but did not avert death in this model, reducing peak bioactive TNF-α levels after infection from 76.4 ng ml^{-1} in control mice to 4.7 ng ml^{-1} in the treated group ($p < 0.05$, two-sample t test). However, these low levels of bioactive TNF-α persisted in the p75 fusion protein–treated animals compared with the controls and were sufficient to mediate delayed death. In contrast, pretreatment with 200 μg of the p55 sTNFR-IgG gave excellent protection against death with complete neutralization of circulating TNF. Studies of the binding of TNF-α with the soluble TNFR fusion proteins showed that the p75 fusion construct exchanges bound TNF-α about 50–100-fold faster than the p55 fusion protein. Thus, although both fusion proteins in equilibrium bind TNF-α with high affinity, the TNF-α p55 fusion protein complex is kinetically more stable than the p75 fusion construct, which thus acts as a TNF carrier. The persistent release of TNF-α from the p75 fusion construct limits its therapeutic effect in this model of sepsis.

Despite significant advances in antibiotic treatment and intensive care management over the last 20 yr, the mortality from sepsis leading to multi-organ failure and septic shock has remained virtually unchanged (1, 2). Infection with a variety of different organisms can produce similar pathophysiological changes within the host through the induction of a number of mediators. Principal among these is TNF-α, a cytokine produced mainly by activated macrophages, which is able in purified form to reproduce nearly all of the features of sepsis and septic shock (3, 4). Neutralization of TNF-α activity may thus be potentially beneficial in the treatment of this condition, and a number of different reagents designed to attenuate TNF-α action have been developed (5).

TNF-α exerts its effects through binding to high affinity cell surface receptors, of which there are two kinds, a 75-(p75) and a 55-kD (p55) form (6–8). These have significant sequence similarity in their extracellular domains, but differ completely in their intracellular portions (9). Many of the effects of TNF-α, including cytotoxicity, are produced by binding to the p55 receptor. This has been demonstrated by the use of agonist antireceptor antibodies (10, 11), and more recently by the use of mice with specific deletion of the p55 receptor gene (12, 13). The role of the p75 receptor is less well defined, but does include effects distinct from those of the p55 receptor, such as stimulating thymocyte proliferation (14). It has also been proposed that the p75 receptor may facilitate TNF-α binding to the p55 receptor, by initial rapid binding of TNF-α which is then subsequently passed to the p55 receptor (15).

TNF-α exists as a trimer in solution, and is potentially able to bind three receptor molecules (16–18). The mechanism by which receptor binding produces the cellular actions of TNF-α is not clear, but a number of experiments have shown that clustering of the p55 receptor is required for TNF-α effects mediated by this receptor (10). Both the p75 and p55 receptors also exist as soluble forms, produced by cleavage of the extracellular domains of the receptors (19, 20). These soluble receptors retain their high affinity binding for TNF-α but do not directly mediate any biological effects. Their production during sepsis may thus be a natural mechanism to attenuate TNF-α action (17, 21).

A number of reagents have been developed to neutralize TNF-α activity. mAbs to TNF-α have shown good activity in a number of animal models of experimental sepsis and are currently undergoing clinical trials (22, 23). Soluble TNF receptors (sTNFR)[1] are an attractive means of attenuating

[1] *Abbreviation used in this paper:* sTNFR-IgG, soluble TNF IgG fusion protein.

TNF action. They have high affinity binding not only for TNF-α, but also TNF-β, a form of TNF produced by activated T cells, which may be of importance in gram-positive infections with toxin-producing organisms (17, 21, 24). By the use of recombinant DNA technology, fusion proteins have been produced in which the soluble part of the TNFR is linked to a human IgG heavy chain constant region to form dimers through the intermolecular disulfide bridges joining normal IgG heavy chains. These dimeric fusion proteins are able to bind to the TNF trimer in two separate sites, thus binding with higher affinity than the natural soluble receptors (17, 21). In addition, the presence of the IgG heavy region confers a longer serum half-life for the fusion protein compared with the soluble receptor alone, with values in excess of 20 h (25, 26).

sTNFR or sTNFR-IgG fusion proteins have been tested in a number of different animal models of sepsis. In baboons challenged with live *Escherichia coli*, treatment with the p55 TNFR was able to improve some of the hemodynamic abnormalities after bacterial challenge, with a suggestion of improved survival in treated animals, although the number of animals used was too small to demonstrate this conclusively (27). A p55 sTNFR-IgG fusion protein was able to protect against death in mice after challenge with LPS (26, 28). However, after intraperitoneal infection in mice, a p55 fusion protein was not able to improve survival, in common with other TNF neutralizing drugs in this particular model (29, 30). p75 fusion proteins have been tested in endotoxemia models of sepsis, where they have been shown to be protective against death in mice injected with LPS (21). However, in one case the fusion protein was shown to function as a carrier for TNF-α, although this did not seem to result in any deleterious effects (21). To better understand which TNFR-IgG fusion protein might be more effective in the therapy of severe sepsis, we have tested the ability of both a p75 and a p55 fusion protein to protect against death in a model of sepsis in mice, using intravenous infection with live *E. coli*. We find that the p55, but not the p75, TNFR-IgG fusion protein was able to provide significant protection against death in this animal model of sepsis.

Materials and Methods

Animals. CD1 mice were used for all experiments and were obtained from Charles Rivers (Margate, UK). Animals weighing between 28 and 32 g were used for all experiments.

Materials. The sTNFR-IgG1 p75 fusion protein was kindly supplied by the Immunex Corporation (Seattle, WA). The sTNFR-IgG3 p55, sTNFR-IgG3 p75, and sTNFR-IgG1 p55 fusion protein have been reported previously (17, 26, 28). The mAb to murine TNF-α (TN3) was kindly provided by Celltech (Slough, UK). Gentamicin was from Roussel Laboratories (Uxbridge, UK). All other materials were from Sigma (Poole, UK).

Bacteria. The bacterial strain used in all experiments was *E. coli* O11:B4 (kindly provided by Dr. Ben Appelmelk, Vrije Universiteit, Amsterdam, The Netherlands). For use in animal experiments, a single bacterial colony was inoculated into No. 2 broth (Oxoid, Basingstoke, UK) and grown for 5.25 h at 37°C. Bacteria were then harvested by centrifugation at 3,000 *g* for 15 min, washed once in sterile pyrogen-free saline, and resuspended in sterile pyrogen-free saline. Bacterial concentration was measured by absorbance at 325 nm and related to previous calibration curves for this organism.

Animal Model of Sepsis. This was performed as described (23). Briefly, animals were inoculated with an LD_{90} of *E. coli* by the tail vein; the inoculum was 3×10^6 CFU per animal. All animals received gentamicin injections intravenously at a dose of 1 mg kg^{-1} at 2 and 5 h after infection, and on each subsequent day a further two i.v. doses at 1 mg kg^{-1}. Treatment with the p75 and p55 sTNFR-IgG fusion proteins was given 30 min before infection by i.v. injection; control animals were given either saline or an equivalent dose of human IgG. No difference in survival was seen in mice injected with either of these control treatments. Endotoxin levels of these protein solutions were <50 pg of endotoxin injected per animal. Mortality was recorded at regular intervals up to 72 h after infection; no mortality was observed after this time in the remaining animals. Blood for cytokine determinations was obtained from the cut tail tip at various times after infection. After clotting, serum was stored at −20°C until assayed.

Cytokine Determinations. TNF-α was measured by bioassay using actinomycin-sensitized L929 cells as described (31). Typically, the lower limit of sensitivity for this assay was ~1 pg ml^{-1}. Serum samples were diluted 267-fold for assay, giving a detection limit in serum of ~267 pg ml^{-1}.

LPS Assay. Endotoxin concentrations were obtained by *Limulus* amebocyte lysate assay using a kit according to the manufacturer's instructions (Chromogenix, Mölndal, Sweden).

Statistical Analysis. Survival curves were compared by the log rank test. Final survival percentages were compared by the two-sample *t* test. Differences in cytokine levels were compared at a given time point by the two-sample *t* test. A result was considered statistically significant if $p < 0.05$.

Dissociation of TNF-α from sTNFR-IgG Fusion Proteins. These experiments were performed with the p55 sTNFR-IgG3, p55 sTNFR-IgG1, and p75 sTNFR-IgG3 constructs reported previously (17, 26). 7.5 μg of the sTNFR-IgG fusion protein was incubated with 2.5 μg TNF-α containing 50 ng ^{125}I-TNF-α (~3 × 10^6 cpm, iodinated according to [32]) in PBS for 20 min on ice. Unbound ^{125}I-TNF-α was separated on a Superose 12 column (Pharmacia, Dübendorf, Switzerland) equilibrated in PBS. The ^{125}I-TNF-α–sTNFR-IgG complexes were collected in a volume of 750 μl and treated with a 50-fold excess of unlabeled TNF-α at room temperature (23°C). 60-μl aliquots were withdrawn at different times and added to 10 μl packed protein G–Sepharose beads (Pharmacia) suspended in 40 μl PBS containing 2% FCS. After 4 min incubation with agitation, the beads were separated by filtrating the sample through a 0.22-μm filter (MC filtration unit; Millipore, Guyancourt, France). The radioactivity in the filtrate and on the filter was measured in a gamma-counter. The time required for quantitative precipitation of the fusion proteins with the protein G–Sepharose beads (4 min) was added to the overall incubation time.

Results

Effect of p75 sTNFR-IgG1 Fusion Protein on Survival. Groups of mice were pretreated either with 250 μg of the p75 sTNFR-IgG1 fusion protein or an equivalent volume of saline 30 min before an LD_{90} i.v. injection of *E. coli*. Survival in these two groups of animals is shown in Fig. 1. Control animals show a steady decrease in survival, starting at 5 h after infection, with a final survival percentage of 11%. The p75 sTNFR-IgG1–treated animals initially were protected against death,

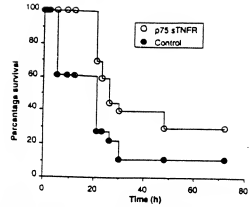

Figure 1. Survival of mice following i.v. infection pretreated with 250 μg of the p75 sTNFR-IgG1 fusion protein (n = 20) 30 min before infection, or with saline (control, n = 18).

with no deaths recorded until 20 h after infection. However, thereafter the mice began to die at the same rate as the control animals, with a final survival percentage of 30% in the p75 sTNFR-IgG1–treated group (Fig. 1). The overall difference in the survival curves between the two groups of mice was statistically significant (p <0.05; log rank test), although the difference between the final survival percentages of 19% was not significant (95% confidence interval ± 22%). This delay in the death of infected mice produced by the p75 sTNFR-IgG1 protein, but with no final protective effect, was highly reproducible, with identical results obtained on two separate occasions. In addition, the same delayed death in p75 sTNFR-IgG–treated animals was obtained compared with control animals which received 250 μg of human IgG. No significant protective effects were seen using lower doses of p75 sTNFR-IgG1 fusion protein (data not shown).

TNF-α Levels after Infection in p75 sTNFR-IgG1–treated Animals. In this model of sepsis, serum TNF-α levels after infection show a peak at 90 min after bacterial inoculation

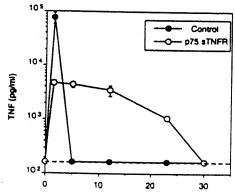

Figure 2. Bioactive serum TNF-α levels after i.v. infection in the animals from the experiment of Fig. 1. Each point is the mean value of sera from three mice. Error bars are ± 1 SEM. The dotted line indicates the lower limit of sensitivity of the cytotoxicity assay.

with undetectable levels of TNF-α at later time points (F 2). The mice treated with the p75 sTNFR-IgG1 prot showed a significant reduction in this peak level of bioact TNF-α from 76.4 ng ml^{-1} in the control animals to 4.7 ml^{-1} in the treated group (p <0.01, two-sample t te However, in contrast to the control animals, bioactive TNF levels in the p75 sTNFR-IgG1–treated mice persisted at t low level for the next 24 h, only becoming undetectable 30 h after infection (Fig. 2).

Role of TNF-α in the Delayed Death of the p75 sTNFR-Ig Animals. We wished to determine whether TNF-α w responsible for the delayed death of the p75 sTNF IgG1–treated mice after bacterial infection, as shown in F 1. To answer this question, we set out to determine whet a neutralizing antibody to TNF-α with known effect in t model (23) could prevent the delayed death in the p75 sTNF IgG1–treated animals. Four groups of 10 mice were all simi taneously infected with an LD_{90} of *E. coli* as before. Ea group received a different treatment. Control-treated anim showed a progressive drop in survival, with a final survi percentage of 10% (Fig. 3, *crosses*). Mice receiving p75 sTNF IgG1 as before showed a delay in death, but with no fi difference in outcome compared with the control group (F 3, *open circles*). The remaining two groups of mice receiv a neutralizing antibody to TNF-α (TN3) at 4 h after infe tion (*arrow* in Fig. 3). When given on its own at this tir after infection, this antibody is unable to protect mice fro death (Fig. 3, *filled squares*), as we have previously shown (2 However, when TN3 was administered at this time in anim that had already received 250 μg of the p75 sTNFR-IgG fusion protein 30 min before infection, the anti-TNF-α an body produced significant protection against death (Fig. *open squares*; p <0.05, log rank test). The low levels of bi active TNF-α that persist in the circulation of the p75 sTNFI

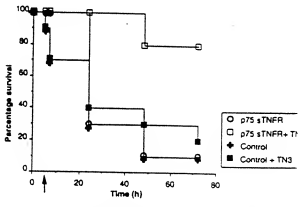

Figure 3. Survival curves of mice after i.v. infection with different trea ment regimens. Control animals received saline at 30 min before infe tion. p75 sTNFR-treated animals received 250 μg of the p75 sTNFR-IgG fusion protein at 30 min before infection. Control plus TN3 animals r ceived the control injection as well as 1 mg of TN3 antibody at 4 h aft infection (*arrow*). p75 sTNFR plus TN3 animals received 250 μg of t p75 sTNFR-IgG1 fusion protein at 30 min before infection as well as mg of the TN3 at 4 h after infection. Each group consisted of 10 mic

IgG1–treated animals are thus responsible for their delayed death.

The reduction in mortality produced by the administration of the TN3 in the p75 sTNFR-IgG1–treated mice is associated with a reduction in the bioactive TNF-α levels (Fig. 4). Animals receiving pretreatment with p75 sTNFR-IgG1 still have measurable bioactive TNF-α levels of 2.2 ng ml^{-1} (SEM 0.67) at 24 h after infection, compared with levels of 0.32 ng ml^{-1} (SEM 0.32) in the mice receiving both the p75 and the TN3 ($p < 0.05$, two-sample t test).

Effect of a Double Dose of the p75 sTNFR-IgG1 Fusion Protein on Mortality. One possible explanation for the lack of efficacy of the p75 sTNFR-IgG1 fusion protein in protecting against death is that an insufficient amount of the reagent was given. To address this question, we treated a group of mice with two doses of the p75 fusion protein: 250 μg was given 30 min before infection as before, and a further 250 μg dose was given at 4 h after bacterial inoculation. There was no difference in the survival of these mice receiving two doses of the p75 sTNFR-IgG1 protein compared with control animals that were infected but that did not receive the fusion protein (data not shown). The animals receiving the double dose of the p75 sTNFR-IgG1 protein still showed the low but persistent levels of bioactive TNF-α in the circulation, as seen with mice receiving a single dose (data not shown).

Effect of p55 sTNFR-IgG1 Fusion Protein on Survival. The effects of the p55 sTNFR-IgG1 fusion protein on survival following i.v. infection of mice with *E. coli* was investigated in exactly the same manner as with the p75 construct. Pretreatment of mice with 50 μg of the p55 sTNFR-IgG1 protein 30 min before bacterial infection gave a significant protection from death compared with control untreated animals (Fig. 5; $p < 0.05$, log rank test). Animals treated with 200 μg of the p55 sTNFR-IgG1 fusion protein produced an enhanced protective effect compared with the lower dose (Fig. 6). The difference in survival between p55 sTNFR-IgG1–treated and control mice was highly significant ($p < 0.01$, log rank test).

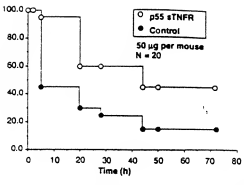

Figure 5. Survival curves of mice after i.v. infection treated with either saline (*Control*) or with 50 μg of the p55 sTNFR-IgG1 fusion protein at 30 min before infection. $n = 20$ for each group.

TNF-α Levels after p55 sTNFR-IgG1 Treatment. The bioactive TNF-α levels in the serum of the mice in this experiment are shown in Fig. 7. At all time points after infection there was no detectable TNF-α in the serum of the p55 sTNFR-IgG1–treated mice, compared with the sharp peak of TNF-α seen at 90 min after infection in the control animals.

Direct Comparison of the p75 and p55 sTNFR-IgG Fusion Proteins. To be certain that the observed differences between the p55 and p75 receptor constructs reflect a real difference in biological efficacy, we compared the ability of the two sTNFR-IgG reagents to protect against death directly within one experiment. A group of 30 mice was divided into three groups of 10 animals. One group received an i.v. injection of saline, another 250 μg of the p75 sTNFR-IgG, and the remaining group 200 μg of the p55 sTNFR-IgG. 30 min later, all animals were inoculated with an LD_{90} of *E. coli*. 72-h survival in the three groups showed 2 out of 10 animals alive in the control group, 1 out of 10 alive in the p75 sTNFR-IgG–treated group, and all 10 animals alive in the p55 sTNFR-IgG–treated group.

Kinetics of TNF-α Binding to p55 and p75 sTNFR-IgG Fusion Proteins. To investigate differences in the biochemical TNF-α binding properties of p55 and p75 TNF receptor-derived fusion proteins, the rate of exchange of TNF-α in

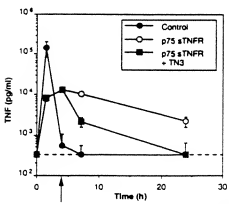

Figure 4. Bioactive TNF-α serum levels in the animals from the experiment described in Fig. 3. Each point is the mean value of sera from three mice determined in cytotoxicity assays. Error bars are ± SEM.

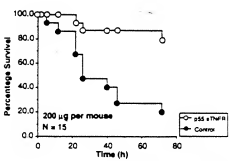

Figure 6. Survival curves of mice after i.v. infection treated with either saline (*Control*) or 200 μg of the p55 sTNFR-IgG1 fusion protein at 30 min before infection. $n = 15$ for each group.

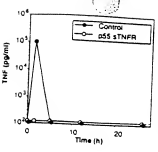

Figure 7. Bioactive TNF-α serum levels in the mice from the experiment described in Fig. 6. Each point is the mean value of sera from three mice determined in cytotoxicity assays. Error bars are ± 1 SEM.

fusion protein–TNF-α complexes was determined (Fig. 8). Briefly, the various fusion proteins were complexed with ^{125}I-TNF-α, placed in buffer containing excess unlabeled TNF-α, and the time-dependent release of ^{125}I-TNF-α was measured. These studies revealed that TNF-α complexed with the p75 sTNFR-IgG exchanged at a significantly higher rate than when complexed with the p55 sTNFR-IgG, as shown by the half-lives of about 7 min for the p75 sTNFR-IgG–TNF-α complex and about 8 h for the p55 sTNFR-IgG–TNF-α complex (Fig. 8).

Discussion

We have shown in the experiments described in this paper that there is a significant difference in the behavior of the p75 and p55 sTNFR-IgG1 fusion proteins in their ability to neutralize TNF-α and protect against death in a murine model of gram-negative sepsis. The p75 construct is able to attenuate the high peak levels of bioactive TNF-α produced after inoculation of mice with *E. coli*, but thereafter these low levels of TNF-α persist in the circulation for many hours and mediate the late death of the mice. The p55 construct, on the other hand, produces complete neutralization of serum TNF-α at all time points after infection, and provides good protection against death in this model of sepsis. The beneficial effect

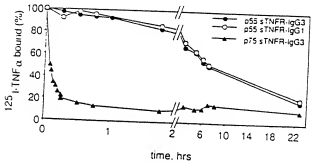

Figure 8. Exchange rates of TNF-α complexed to p55 and p75 sTNFR Ig fusion proteins. ^{125}I-TNF-α was allowed to bind to the various fusion proteins and at time zero an excess of unlabeled TNF-α was added. The exchange of ^{125}I-TNF-α with unlabeled TNF-α was measured at different times as indicated using protein G–Sepharose beads to separate receptor-bound from free TNF-α. 100% complexed ^{125}I-TNF-α was determined in the absence of unlabeled TNF-α. Note the different time scales in left and right panels.

of the p55 sTNFR-IgG construct on survival compared wit the p75 construct was highly reproducible between exper ments and, importantly, could be demonstrated when th two reagents were compared directly within one experiment

The delay in death produced by the p75 sTNFR-IgG1 fu sion protein in the model used in the experiments describe here was sufficient to produce a statistically significant differ ence between the survival curves for treated and control group of mice, although the final outcome was similar between th two groups and not significantly different (Fig. 1). The bio active TNF-α levels in these animals provide an explanatio for this result. The p75 sTNFR-IgG1 protein is able to at tenuate the peak TNF-α levels after bacterial inoculation, but thereafter acts as a carrier for TNF-α, which persists in the circulation at low levels until 30 h after infection, in contrast to the very rapid disappearance of TNF-α in the control animals (Fig. 2). This ability of the p75 sTNFR-IgG1 protein to act as a carrier for TNF-α has been observed in mice after experimental endotoxemia (21).

The release of bioactive TNF-α from the p75 sTNFR-IgG1 to produce low but persistent levels of this cytokine up to 30 h after infection is sufficient to produce the delayed death in these animals. This is demonstrated by the ability of a neutralizing mAb to TNF-α (TN3) administered 4 h after infection to protect the p75 sTNFR-IgG1–treated animals (Fig. 3). When administered at this time point, the TN3 is ineffective at protecting against death on its own, presumably because the peak of TNF-α has already passed (Fig. 4, control animals). The TN3 antibody also reduces the circulating bioactive TNF-α levels compared with the mice receiving the p75 sTNFR-IgG1 fusion protein alone (Fig. 4).

Why does the TNF-α carried by the p75 sTNFR-IgG fusion protein produce a deleterious effect in the model of gram-negative sepsis described here, but is not harmful after endotoxin challenge in mice (21)? There are several possible explanations. The TNF-α levels produced after bacterial challenge in the model used in our experiments are much higher. Mice typically have peak levels of ~80 ng ml^{-1} after bacterial infection (Fig. 2) compared with the levels of ~0.5 ng ml^{-1} reported after endotoxin challenge in mice (21). In addition, i.v. challenge with live bacteria is a considerably more complex stimulus than LPS challenge alone. For example, the LPS-resistant mouse strain C3H/HeJ is as susceptible to i.v. challenge with live *E. coli* as its parent strain, C3H/HeN, despite an enormous difference in susceptibility after LPS challenge (33). Finally, in producing a lethal effect in animals, TNF-α synergizes strongly with other cytokines such as IFN-γ which are produced at high levels in the model of sepsis used in the experiments reported here (34, and data not shown).

An important consideration in the experiments with the p75 sTNFR-IgG protein is that the results obtained might be dependent on the exact stoichiometry of binding of the p75 fusion protein with TNF-α. In vitro, the carrier functions of soluble TNFR have been demonstrated at low ratios of receptor to TNF, at higher soluble receptor concentrations, the neutralizing properties predominate (35). However, the administration of a second identical dose of the p75

fusion protein at 4 h after infection in animals that had already received 250 μg 30 min before bacterial inoculation did not improve survival. In addition, this double dose of p75 sTNFR-IgG1 fusion protein did not alter substantially the prolonged presence of bioactive TNF-α in the serum of the infected animals. This is in marked contrast to the effect of TN3 described above and shows that prolonged presence of bioactive TNF-α in the serum of the p75 sTNFR-IgG1-treated mice is not due to inadequate dosing of the fusion protein.

In contrast to the p75 sTNFR-IgG1 fusion protein, the p55 sTNFR-IgG1 protein provides good protection against death in this model of sepsis (Fig. 6). The protective effect is dependent on the dose of the administered p55 material. At 50 μg per mouse, the protective effect was much more modest than that seen with a 200 μg per animal dose (Figs. 5 and 6). With a dose of 200 μg of p55 sTNFR-IgG1 protein given 30 min before infection, complete neutralization of circulating bioactive TNF-α was produced (Fig. 7). The specificity of the beneficial effect on survival of the p55 reagent is shown by the lack of benefit seen in animals injected with either saline, human IgG, or the p75 sTNFR-IgG construct.

Why should there be this difference between the p55 and p75 reagents? In many respects the p55 and p75 sTNFR-IgG1 fusion proteins have similar properties. They both bind TNF-α in solution with similar high equilibrium binding constants (17, 21). The elimination half-life of both reagents is very similar, in the order of 20 h (25, 26). However, one possible explanation for their different effects in this model of sepsis is their different kinetics of TNF-α binding and release. The p75 sTNFR-IgG fusion protein binds and releases TNF-α ~100-fold faster than the p55 fusion protein (Fig. 8). The different binding kinetics of p55 and p75 sTNFR-IgG reflect inherent properties of the p55 and p75 TNFR molecules that carry over into the fusion protein constructs (36, and Loetscher, H., D. Belluoccio, and W. Lesslauer, unpublished data). Thus although the p75 fusion protein under equilibrium conditions has the same affinity as the p55 construct, it is less kinetically stable. This has a profound influence on the partitioning of TNF-α between fusion protein, natural soluble and membrane bound TNFR in blood, as reflected by the different TNF-α concentrations revealed in the cytotoxicity assays. The difference in outcome of the p55 and p75 sTNFR-IgG1 treatments thus may be understood from the different binding kinetics of the two constructs.

What are the therapeutic implications of these results? Results from animal models must be interpreted cautiously before extrapolation to human disease. However, the experiments described here do demonstrate an important difference in the biological properties of the two sTNFR-IgG fusion proteins. The protective effects of the p55 construct compared with the p75 protein in the model of sepsis used in our experiments suggest that the p55 sTNFR-IgG will also be more likely to be effective in human disease.

This work was supported by the Medical Research Council, UK through the award of a Medical Research Council Clinician/Scientist Research fellowship to T. J. Evans.

Address correspondence to Professor J. Cohen, Department of Infectious Diseases and Bacteriology, Royal Postgraduate Medical School, Du Cane Road, London W12 0NN, UK.

Received for publication 22 June 1994 and in revised form 15 August 1994.

References

1. Rackow, E.C., and M.E. Astiz. 1991. Pathophysiology and treatment of septic shock. *J. Am. Med. Assoc.* 266:548.
2. Glauser, M.P., G. Zanetti, J.-D. Baumgartner, and J. Cohen. 1991. Septic shock: pathogenesis. *Lancet.* 338:732.
3. Tracey, K.J., B. Beutler, S.F. Lowry, J. Merryweather, S. Wolpe, I.W. Milsark, R.J. Hariri, T.J. Fahey III., A. Zentella, J.D. Albert, et al. 1986. Shock and tissue injury induced by recombinant human cachectin. *Science (Wash. DC).* 234:470.
4. Michie, H.R., K.R. Manogue, D.R. Spriggs, A. Revhaug, S. O'Dwyer, C. Dinarello, A. Cerami, S.M. Wolff, and D.W. Wilmore. 1988. Detection of circulating tumour necrosis factor after endotoxin administration. *N. Engl. J. Med.* 318:1481.
5. Dinarello, C.A., J.A. Gelfand, and S.M. Wolff. 1993. Anticytokine strategies in the treatment of the systemic inflammatory response syndrome. *J. Am. Med. Assoc.* 269:1829.
6. Loetscher, H., Y.-C.E. Pan, H.-W. Lahm, R. Gentz, M. Brockhaus, H. Tabuchi, and W. Lesslauer. 1990. Molecular cloning and expression of the human 55kd tumor necrosis factor receptor. *Cell.* 61:351.
7. Schall, T.J., M. Lewis, K.J. Koller, A. Lee, G.C. Rice, G.H.W. Wong, T. Gatanaga, G.A. Granger, R. Lentz, H. Raab, et al. 1990. Molecular cloning and expression of a receptor for human tumor necrosis factor. *Cell.* 61:361.
8. Smith, C.A., T. Davis, D. Anderson, L. Solam, M.P. Beckmann, R. Jerzy, S.K. Dower, D. Cosman, and R.G. Goodwin. 1990. A receptor for tumor necrosis factor defines an unusual family of cellular and viral proteins. *Science (Wash. DC).* 248:1019.
9. Dembic, Z., H.R. Loetscher, U. Gubler, Y.-C.E. Pan, H.-W. Lahm, R. Gentz, M. Brockhaus, and W. Lesslauer. 1990. Two human TNF receptors have similar extracellular, but distinct intracellular, domain sequences. *Cytokine.* 2:231.
10. Engelmann, H., H. Holtmann, C. Brakebusch, Y.-S. Avni, I. Sarov, Y. Nophar, E. Hadas, O. Leitner, and D. Wallach.

1990. Antibodies to a soluble form of a tumor necrosis factor (TNF) receptor have TNF-like activity. *J. Biol. Chem.* 265:14497.
11. Espevik, T., M. Brockhaus, H. Loetscher, U. Nonstad, and R. Shalaby. 1990. Characterization of binding and biological effects of monoclonal antibodies against a human tumor necrosis factor receptor. *J. Exp. Med.* 171:415.
12. Pfeffer, K., T. Matsuyama, T.M. Kündig, A. Wakeham, K. Kishihara, A. Shahinian, K. Wiegmann, P.S. Ohashi, M. Krönke, and T.W. Mak. 1993. Mice deficient for the 55kd tumor necrosis factor receptor are resistant to endotoxic shock, yet succumb to *L. monocytogenes* infection. *Cell.* 73:457.
13. Rothe, J., W. Lesslauer, H. Lötscher, Y. Lang, P. Koebel, F. Köntgen, A. Althage, R. Zinkernagel, M. Steinmetz, and H. Bluethmann. 1993. Mice lacking the tumour necrosis factor receptor 1 are resistant to TNF-mediated toxicity but highly susceptible to infection with *Listeria monocytogenes*. *Nature (Lond.).* 364:798.
14. Tartaglia, L., R.F. Weber, I.S. Figari, C. Reynolds, M.A. Palladino, Jr., and D.V. Goeddel. 1991. The two different receptors for tumor necrosis factor mediate distinct cellular responses. *Proc. Natl. Acad. Sci. USA.* 88:9292.
15. Tartaglia, L.A., and D.V. Goeddel. 1992. Two TNF receptors. *Immunol. Today.* 13:151.
16. Eck, M.J., and S.R. Sprang. 1989. The structure of tumor necrosis factor alpha at 2.6 Å resolution: implications for receptor binding. *J. Biol. Chem.* 264:17595.
17. Loetscher, H., R. Gentz, M. Zulauf, A. Lustig, H. Tabuchi, E.-J. Schlaeger, M. Brockhaus, H. Gallati, M. Manneberg, and W. Lesslauer. 1991. Recombinant 55-kDa tumor necrosis factor (TNF) receptor. *J. Biol. Chem.* 266:18324.
18. Pennica, D., V.T. Lam, R.F. Weber, W.J. Kohr, L.J. Basa, M.W. Spellman, A. Ashkenazi, S.J. Shire, and D.V. Goeddel. 1993. Biochemical characterization of the extracellular domain of the 75-kilodalton tumor necrosis factor receptor. *Biochemistry.* 32:3131.
19. Engelmann, H., D. Novick, and D. Wallach. 1990. Two tumor-necrosis factor-binding proteins purified from human urine. Evidence for immunological cross-reactivity with cell surface tumor necrosis factor receptors. *J. Biol. Chem.* 265:1531.
20. Nophar, Y., O. Kemper, C. Brakebusch, H. Engelmann, R. Zwang, D. Aderka, H. Holtmann, and D. Wallach. 1990. Soluble forms of tumor necrosis factor receptors (TNF-Rs). The cDNA for the type I TNF-R, cloned using amino-acid sequence data of its soluble form, encodes both the cell surface and a soluble form of the receptor. *EMBO (Eur. Mol. Biol. Organ.) J.* 9:3269.
21. Mohler, K.M., D.S. Torrance, C. Smith, R.G. Goodwin, K.E. Stremler, V.P. Fung, H. Madani, and M.B. Widmer. 1993. Soluble tumor necrosis factor (TNF) receptors are effective therapeutic agents in lethal endotoxemia and function simultaneously as both TNF carriers and TNF antagonists. *J. Immunol.* 151:1548.
22. Tracey, K.J., Y. Fong, D.G. Hesse, K.R. Manogue, A.T. Lee, G.C. Kuo, S.F. Lowry, and A. Cerami. 1987. Anti-cachectin/TNF monoclonal antibodies prevent septic shock during lethal bacteraemia. *Nature (Lond.).* 330:662.
23. Silva, A.T., K.F. Bayston, and J. Cohen. 1990. Prophylactic and therapeutic effects of a monoclonal antibody to tumour necrosis factor-alpha in experimental Gram-negative shock. *J. Infect. Dis.* 162:421.
24. Hackett, S.P., and D.L. Stevens. 1993. Superantigens associate with Staphylococcal and Streptococcal toxic shock syndrom are potent inducers of tumor necrosis factor-β synthesis. *J. I fect. Dis.* 168:232.
25. Jacobs, C.A., M.P. Beckmann, K. Mohler, C.R. Maliszewsk W.C. Fanslow, and D.H. Lynch. 1993. Pharmacokinet parameters and biodistribution of soluble cytokine receptor *Int. Rev. Exp. Pathol.* 34B:123.
26. Lesslauer, W., H. Tabuchi, R. Gentz, M. Brockhaus, E.J Schlaeger, G. Grau, P.F. Piguet, P. Pointaire, P. Vassalli, an H. Loetscher. 1991. Recombinant soluble tumor necrosis facto receptor proteins protect mice from lipopolysaccharide-induce lethality. *Eur. J. Immunol.* 21:2883.
27. Van Zee, K.J., T. Kohno, E. Fischer, C.S. Rock, L.L. Mol dawer, and S. Lowry. 1992. Tumor necrosis factor soluble receptors circulate during experimental and clinical inflamma tion and can protect against excessive tumor necrosis factor α *in vitro* and *in vivo*. *Proc. Natl. Acad. Sci. USA.* 89:4845.
28. Ashkenazi, A., S.A. Marsters, D.J. Capon, S.M. Chamow, I.S. Figari, D. Pennica, D.V. Goeddel, M.A. Palladino, and D.H. Smith. 1991. Protection against endotoxic shock by a tumor necrosis factor receptor immunoadhesion. *Proc. Natl. Acad. Sci. USA.* 88:10535.
29. Angehrn, P., D. Banner, T. Braun, A. d'Arcy, G. Gehr, R. Gentz, F. Mackay, E.-J. Schlaeger, H. Schoenfeld, H. Loetscher, and W. Lesslauer. 1993. Two distinct tumor necrosis factor receptors in health and disease. *In* Tumor Necrosis Factor: Molecular and Cellular Biology and Clinical Relevance. W. Fiers and W.A. Buurman, editors. Karger, Basel. 33–39.
30. Echtenacher, B., W. Falk, D.N. Männel, and P.H. Krammer. 1990. Requirement of endogenous tumor necrosis factor/cachectin for recovery from experimental peritonitis. *J. Immunol.* 145:3762.
31. Flick, D.A., and G.E. Gifford. 1984. Comparison of in vitro cell cytotoxic assays for tumor necrosis factor. *J. Immunol. Methods.* 68:167.
32. Brockhaus, M., H.-J. Schoenfeld, H.-J. Schlaeger, W. Hunziker, W. Lesslauer, and H. Loetscher. 1990. Identification of two kinds of TNF receptors on human cell lines by monoclonal antibodies. *Proc. Natl. Acad. Sci. USA.* 87:3127.
33. Evans, T.J., E. Strivens, A. Carpenter, and J. Cohen. 1993. Differences in cytokine response and induction of nitric oxide synthase in endotoxin-resistant and endotoxin-sensitive mice after intravenous Gram-negative infection. *J. Immunol.* 150:5033.
34. Evans, T., A. Carpenter, A. Silva, and J. Cohen. 1992. Differential effects of monoclonal antibodies to tumor necrosis factor alpha and gamma interferon on induction of hepatic nitric oxide synthase in experimental Gram-negative sepsis. *Infect. Immun.* 60:4133.
35. Aderka, D., H. Engelmann, Y. Maor, C. Brakebusch, and D. Wallach. 1992. Stabilization of the bioactivity of tumor necrosis factor by its soluble receptors. *J. Exp. Med.* 175:323.
36. Tartaglia, L.A., D. Pennica, and D.V. Goeddel. 1993. Ligand passing: the 75-kDa tumor necrosis factor (TNF) receptor recruits TNF for signalling by the 55-kDa TNF receptor. *Proc. Natl. Acad. Sci. USA.* 268:18542.

Recombinant 55-kDa Tumor Necrosis Factor (TNF) Receptor

STOICHIOMETRY OF BINDING TO TNFα AND TNFβ AND INHIBITION OF TNF ACTIVITY*

(Received for publication, February 21, 1991)

Hansruedi Loetscher‡§, Reiner Gentz‡, Martin Zulauf‡, Ariel Lustig¶, Hisahiro Tabuchi‖, Ernst-Juergen Schlaeger‡, Manfred Brockhaus‡, Harald Gallati‡, Michael Manneberg‡, and Werner Lesslauer‡

From the ‡Pharma Research New Technologies, F. Hoffmann-LaRoche Ltd., CH-4002 Basel, Switzerland, the ¶Biocenter, University of Basel, CH-4056 Basel, Switzerland, and the ‖Nippon Roche Research Center, Department of Molecular Genetics, Kamakura, Kanagawa 247, Japan

The extracellular domain of the 55-kDa TNF receptor (rsTNFRβ) has been expressed as a secreted protein in baculovirus-infected insect cells and Chinese hamster ovary (CHO)/dhfr⁻ cells. A chimeric fusion protein (rsTNFRβ-hγ3) constructed by inserting the extracellular part of the receptor in front of the hinge region of the human IgG Cγ3 chain has been expressed in mouse myeloma cells. The recombinant receptor proteins were purified from transfected cell culture supernatants by TNFα- or protein G affinity chromatography and gel filtration. In a solid phase binding assay rsTNFRβ was found to bind TNFα with high affinity comparable with the membrane-bound full-length receptor. The affinity for TNFβ was slightly impaired. However, the bivalent rsTNFRβ-hγ3 fusion protein bound both ligands with a significantly higher affinity than monovalent rsTNFRβ reflecting most likely an increased avidity of the bivalent construct. A molecular mass of about 140 kDa for both rsTNFRβ·TNFα and rsTNFRβ·TNFβ complexes was determined in analytical ultracentrifugation studies strongly suggesting a stoichiometry of three rsTNFRβ molecules bound to one TNFα or TNFβ trimer. Sedimentation velocity and quasielastic light scattering measurements indicated an extended structure for rsTNFRβ and its TNFα and TNFβ complexes. Multiple receptor binding sites on TNFα trimers could also be demonstrated by a TNFα-induced agglutination of Latex beads coated with the rsTNFRβ-hγ3 fusion protein. Both rsTNFRβ and rsTNFRβ-hγ3 were found to inhibit binding of TNFα and TNFβ to native 55- and 75-kDa TNF receptors and to prevent TNFα and TNFβ bioactivity in a cellular cytotoxicity assay. Concentrations of rsTNFRβ-hγ3 equimolar to TNFα were sufficient to neutralize TNF activity almost completely, whereas a 10–100-fold excess of rsTNFRβ was needed for similar inhibitory effects. In view of their potent TNF antagonizing activity, recombinant soluble TNF receptor fragments might be useful as therapeutic agents in TNF-mediated disorders.

Tumor necrosis factor (TNF)[1] α and β are two closely related cytokines with about 30% sequence homology (1–3). Their genes are closely linked in the major histocompatibility complex of mammals (4). TNFα and TNFβ are primarily produced by activated macrophages and lymphocytes, respectively (5, 6). Based on crystallographic (7, 8) and analytical centrifugation studies (9) both cytokines are believed to form trimers. A wide variety of TNFα and TNFβ activities *in vitro* has been described including growth enhancement of fibroblasts (10), growth inhibition or lysis of some transformed cells (11), differentiation of human myeloid cell lines (12), and induction of the expression of cell surface molecules (13–15). *In vivo* TNFα induces hemorrhagic necrosis of certain transplantable tumors (16, 17), is involved in immune and inflammatory reactions (18–20), and mediates lethal effects in endotoxin-induced septic shock (21–23).

We have identified two human TNF receptors of about 75- and 55-kDa apparent molecular masses (in the present paper called TNFRα and TNFRβ, respectively) by chemical cross-linking with radiolabeled TNFα (24) and by binding of monoclonal antibodies generated against isolates of the receptors (25). Subsequently, both receptors have been purified from HL60 cells and partial amino acid sequences were determined (26). More recently, the cDNAs of TNFRα and TNFRβ were isolated by us (27, 28) and several other groups (29–34). The two receptors show similar cysteine-rich motifs in their extracellular domains and belong to a new cytokine receptor gene family which includes the nerve growth factor receptor, CD40, and OX40 antigens (28, 35).

Soluble fragments of both TNF receptors have been found to be present in human serum and urine (36–40). In certain disease states receptor shedding appears to be increased (40, 41). Soluble TNF receptors have also been identified in cell culture medium of some transformed cell lines (32, 42) and of stimulated polymorphonuclear leukocytes (43). In functional studies the natural TNF receptor fragments have been shown to protect cells from TNFα-induced cytotoxicity (36–39) and, in a recent report, to prevent TNFα-induced hemorrhagic necrosis of a transplanted Meth A sarcoma in BALB/c mice (40). The TNF-antagonizing effects of the soluble receptor fragments *in vitro* and *in vivo* imply a specific interaction with TNFα and TNFβ which might be an important regulatory mechanism of TNF action.

* The costs of publication of this article were defrayed in part by the payment of page charges. This article must therefore be hereby marked "*advertisement*" in accordance with 18 U.S.C. Section 1734 solely to indicate this fact.

§ To whom correspondence should be addressed: Pharma Research New Technologies, F. Hoffmann-LaRoche Ltd., PRTB, Bldg. 15/40, CH-4002 Basel, Switzerland. Tel.: 61-6883259; Fax: 691-9391

[1] The abbreviations used are: TNF, tumor necrosis factor; TNFRα, 75-kDa TNF receptor; TNFRβ, 55-kDa TNF receptor; rsTNFRβ, recombinant soluble TNFRβ; rsTNFRβ-hγ3, recombinant soluble TNFRβ-human IgG Cγ3 fusion protein; PBS, phosphate-buffered saline; SDS-PAGE, sodium dodecyl sulfate-polyacrylamide gel electrophoresis; CHO, Chinese hamster ovary.

In the present work a recombinant soluble form of the 55-kDa TNF receptor (rsTNFRβ) was produced in high yields in different eukaryotic expression systems. The rsTNFRβ was also expressed as a human IgG Cγ3 fusion protein (rsTNFRβ-hγ3) in myeloma cells. The recombinant receptor molecules were found to bind stoichiometrically to TNFα and TNFβ trimers and to neutralize TNF bioactivity in different assay systems.

EXPERIMENTAL PROCEDURES

Cell Lines and Reagents—The *Spodoptera frugiperda* (Sf9) cell line was obtained from American Type Culture Collection (ATCC CRL 1711). The baculovirus *Autographa californica* (AcNP virus) was obtained from M. Summers, Texas A & M University, the Chinese hamster ovary (CHO)/dhfr⁻ cell line from P. Familetti, Hoffmann-LaRoche Ltd., Nutley, NJ, and the WEHI164 (clone 2A3) cell line from J. R. Frey (51). The mouse myeloma cell line J558L was kindly provided by A. Traunecker, Basel Institute of Immunology. The expression vector used to construct the rsTNFRβ-hγ3 fusion protein was modified from a CD4-immunoglobulin construct obtained from K. Karjalainen and A. Traunecker (44). Recombinant human TNFα and TNFβ and mouse TNFα produced in *Escherichia coli* were kindly provided by W. Hunziker, H.J. Schoenfeld, and E. Hochuli (Hoffmann-LaRoche Ltd.,Basel). Radioiodination of TNFα and TNFβ was performed with $Na^{125}I$ and Iodo-Gen (Pierce Chemical Co.) as described (25). For affinity column chromatography TNFα was coupled to CNBr-activated Sepharose 4B (Pharmacia LKB Biotechnology Inc.) according to the guidelines of the manufacturer. Protein G-Sepharose 4 Fast Flow was purchased from Pharmacia. Latex beads (polystyrene microspheres, 0.48 μm diameter) were originally obtained from Polysciences, Inc., Warrington, PA and kindly provided by R. Spinnler and M. Caravatti (Hoffmann-LaRoche Ltd., Basel, Diagnostic Division).

Construction of Vectors, Expression, and Purification—The cDNA encoding the extracellular domain of TNFRβ, including the signal peptide, was amplified by the polymerase chain reaction. Unique restriction sites were introduced at both ends of the fragment. In addition, a translational stop codon was introduced behind the last amino acid of the extracellular domain (Thr^{+182}, numbering according to Ref. 27). The engineered fragment was cloned into an expression vector for mammalian cells. The plasmid contained the Rous sarcoma virus long terminal repeat and the 3′ intron plus the polyadenylation site from the rat preproinsulin gene. The expression cassette was finally inserted into the *Pvu*II restriction site of plasmid pSV2-DHFR. Transfected CHO/dhfr⁻ cells were initially selected by the neomycin analogue G418 in α-medium containing 200 nmol/ml methotrexate. Thereafter, the concentration of methotrexate was sequentially increased by 2-5-fold increments up to 150 μmol/ml. For expression in the baculovirus system, homologous recombination was used to introduce the amplified cDNA fragment into the genome of the AcNP virus. Sf9 cells were grown at 27 °C in EX-CELL 400 medium (J. R. Scientific, Woodland, CA) containing 2% fetal bovine serum. Cell culture and viral infection were carried out as described (45). The recombinant viruses were purified by limited dilutions in microtiter plates followed by dot blot hybridization. The rsTNFRβ-hγ3 fusion protein was constructed by exchanging the CD4 sequence in the pCD4-hγ3–4 vector (44) with the TNFRβ extracellular domain sequence using *Sst* restriction sites. This procedure yielded a chimeric protein in which the TNFRβ sequence was inserted in front of the hinge region of the human IgG Cγ3 chain. J558L mouse myeloma cells transfected with the rsTNFRβ-hγ3 construct by protoplast fusion were cultured in DHI medium (Dulbecco's modified Eagle's medium/Ham's F-12/Iscove's modified Dulbecco's medium, 25/25/50) supplemented with selenite (20 nM), ethanolamine (20 μM), insulin (5 μg/ml), human transferrin (6 μg/ml), Primatone RL (2.5 mg/ml), Pluronic F68 (0.1 mg/ml), and 0–2% fetal calf serum (46). Expression of rsTNFRβ and rsTNFRβ-hγ3 was analyzed by a sandwich-type binding assay using radiolabeled or peroxidase-labeled TNFα and the non-neutralizing monoclonal antibody htr-20 (25).

Cell-free supernatants of cell transfectant cultures containing rsTNFRβ or rsTNFRβ-hγ3 were concentrated 5-10-fold by ultrafiltration (molecular mass cutoff of 10 kDa) and clarified by centrifugation and filtration through a 0.45-μm filter. The clear filtrate was applied to a TNFα affinity column (Sf9 and CHO/dhfr⁻ supernatants) or protein G affinity column (J558L supernatants). After extensive washing with phosphate-buffered saline (PBS) the columns were eluted with 1 M glycine, 100 mM NaCl, pH 2.6, buffer. The fractions containing the recombinant proteins were concentrated and subjected to gel filtration chromatography on TSK3000SW or Superose 12 (Pharmacia) columns with PBS as solvent. The amount of protein was determined by amino acid analysis or BCA assay (Pierce). Sodium dodecyl sulfate-polyacrylamide gel electrophoresis (SDS-PAGE) was performed as described (47) using the mini-gel system of Bio-Rad.

Binding Assay and Scatchard Analysis—A 96-well microtiter plate coated with the TNFRβ-specific non-neutralizing monoclonal antibody htr-20 (25) was incubated with 10 ng/ml rsTNFRβ or rsTNFRβ-hγ3 in 1% defatted milk powder for 3 h at room temperature. Under these conditions only about 10% of the total binding sites were occupied by the receptor protein as determined from a titration curve (low density packing). In some experiments the antibody-coated plate was incubated with 3 μg/ml soluble receptor to saturate all receptor binding sites (high or maximum density packing). After washing with PBS the wells were incubated with different concentrations of radiolabeled TNFα or TNFβ (1–250 ng/ml) in the presence or absence of a 200-fold excess unlabeled ligand for 16 h at 4 °C. The radioactivity bound to single wells was directly counted in a γ-counter. Nonspecific binding was subtracted. K_d values were determined from Scatchard plots.

Quasielastic Light Scattering and Ultracentrifugation Analysis—Quasielastic light scattering experiments were performed with the system ALV-300 (ALV Laservertriebsges m.b.H., Langen, Germany). Samples of 300 μl were filtered through 0.2-μm filters in closed cylindrical quartz cells. The protein concentration was 0.5–1 mg/ml. Correlation functions were analyzed with the program CONTIN (48) that yields a distribution of relaxations. Mean values for the diffusion coefficient D were calculated assuming either an extended, *i.e.* rod-like (0 moment of the observed distribution) or roughly spherical structure (3rd moment) of the particles.

A Beckman Model E centrifuge with a AnD rotor and a 12-mm double sector Epon cell was used for analytical centrifugation studies. The rotor was run at 56,000 rpm in the sedimentation velocity experiments and at 24,000 or 11,000 rpm in the sedimentation equilibrium experiments. All runs were performed at room temperature using aliquots of the solutions investigated by quasielastic light scattering. Relative mole masses were calculated from the observed sedimentation velocities by the Svedberg equation using the mean values of the diffusion coefficients as described above. The partial specific volume of rsTNFRβ was assumed to be 0.68 ml/g taking into account 30% glycosylation (w/w) (49). Alternatively, the molecular masses were also obtained from the sedimentation equilibrium runs by analyzing the absorption as a function of the square radius (50).

Competitive Inhibition of Ligand Binding to Native TNFRβ and TNFRα Holoreceptors—1–2 ng of native TNFRβ and TNFRα purified from HL60 cells (26) were spotted to prewetted nitrocellulose membranes. After blocking with a solution of 1% defatted milk powder, the membrane was incubated with human radiolabeled TNFα or TNFβ (1 pmol/ml) in the presence of different concentrations of rsTNFRβ or rsTNFRβ-hγ3 for 2 h at room temperature. The membrane was then thoroughly rinsed with PBS and counted in a γ-counter.

WEHI164 Cytotoxicity Assay—WEHI164 cells (clone 2A3, kindly provided by J. R. Frey (51)) were cultured in a microtiter plate at 10⁴ cells/well in a RPMI-based medium in the presence of human TNFα or TNFβ and different concentrations of rsTNFRβ or rsTNFRβ-hγ3 for 48 hours at 37 °C. Cell viability was determined by a dye uptake method as described earlier (9).

Agglutination of Latex Beads—5 mg of Latex beads washed with PBS, pH 5.0, buffer and H_2O were incubated with 250 μg of rsTNFRβ-hγ3 in 0.5 ml of PBS, pH 5.0, overnight at 4 °C on a rotating wheel. The beads were then treated with a solution of 1% defatted milk powder to block any remaining binding sites and washed with PBS buffer. To induce agglutination the beads were suspended at 0.2–1.0 mg/ml in PBS, pH 7.4, containing 0.1 mg/ml bovine serum albumin and 0.1% NaN_3. Human TNFα was added at different concentrations and after overnight incubation at room temperature agglutination was analyzed in a light microscope at × 400 magnification.

RESULTS

Expression, Purification, and Ligand Binding Affinities of rsTNFRβ—Sf9 insect cells infected with the recombinant baculovirus secreted 5–10 μg/ml of soluble receptor into the

medium after 3–5 days in culture. Transfected CHO/dhfr$^-$ cells produced up to 30 μg/ml of the recombinant protein after amplification in the presence of increasing methotrexate concentrations. The TNFRβ-hy3 fusion protein was expressed and secreted in mouse myeloma cells with a yield of about 0.5–1 μg/ml.

The recombinant soluble TNF receptors were purified by TNFα or protein G affinity chromatography and gel filtration. SDS-PAGE analysis revealed for the baculovirus expressed protein three to four discrete bands between 21 and 25 kDa. When virus-infected Sf9 cells were cultured in the presence of tunicamycin, however, a single protein species of 21 kDa was obtained (see Fig. 1) which also was the only TNFα-reacting band in a ligand blot experiment (not shown). N-terminal sequence analysis of the glycosylated baculovirus-produced material revealed a single sequence starting with Leu^{+1} of the mature TNFRβ (not shown). rsTNFRβ produced in CHO/dhfr$^-$ cells yielded two bands migrating on SDS gels at around 28 and 32 kDa. Sequence analysis of this material confirmed the expected N terminus, but a second N-terminal sequence starting at Asp^{+12} was also present in a roughly 1:1 ratio. Interestingly, Asp^{+12} has previously been found to be the N terminus of the naturally occurring TNFRβ fragment (36). The TNFRβ-hy3 fusion protein was expressed as a disulfide-linked homodimer indicating an antibody-like structure of this molecule. As shown in Fig. 1 reduced samples of baculovirus- or CHO/dhfr$^-$-derived rsTNFRβ migrated at a slightly lower rate on SDS gels. This is most likely due to the high content of cysteines in these proteins. A similar observation has been made earlier with the native 55-kDa TNFRβ purified from HL60 cells (26).

The soluble receptor fragments produced in either expression system showed a high affinity for TNFα and a slightly lower affinity for TNFβ (see Fig. 2). The difference in the apparent K_d values of rsTNFRβ for TNFα and TNFβ was most prominent with the CHO/dhfr$^-$-derived material. This finding is in contrast to the native cell surface-bound 55-kDa TNFRβ, which has been shown to bind both TNFα and TNFβ with about the same affinity, i.e. K_d values of 326 and 351 pM, respectively (24, 52)). Interestingly, fully deglycosylated rs-TNFRβ as expressed in baculovirus-infected Sf9 cells in the presence of tunicamycin displayed similar binding characteristics as the glycosylated form (data not shown), confirming that the carbohydrate moieties are not essential for ligand

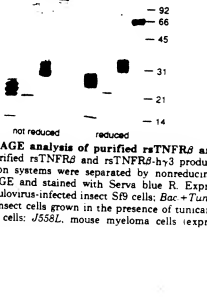

FIG. 1. **SDS-PAGE analysis of purified rsTNFRβ and rs-TNFRβ-hy3.** Purified rsTNFRβ and rsTNFRβ-hy3 produced in different expression systems were separated by nonreducing and reducing SDS-PAGE and stained with Serva blue R. Expression systems: *Bac.*, baculovirus-infected insect Sf9 cells; *Bac.+Tun.*, baculovirus-infected insect cells grown in the presence of tunicamycin; *CHO*, CHO/dhfr$^-$ cells; *J558L*, mouse myeloma cells (expressing rsTNFRβ-hy3).

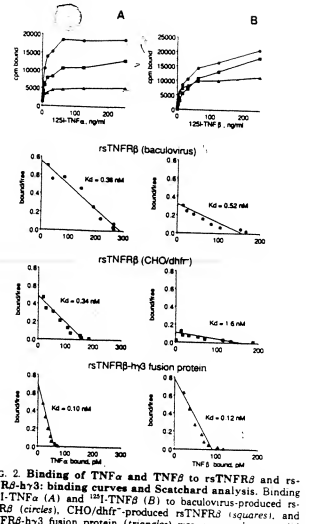

FIG. 2. **Binding of TNFα and TNFβ to rsTNFRβ and rs-TNFRβ-hy3: binding curves and Scatchard analysis.** Binding of ^{125}I-TNFα (*A*) and ^{125}I-TNFβ (*B*) to baculovirus-produced rs-TNFRβ (*circles*), CHO/dhfr$^-$-produced rsTNFRβ (*squares*), and rsTNFRβ-hy3 fusion protein (*triangles*) was measured in a solid phase assay under low density packing conditions (see "Experimental Procedures"). The K_d values were determined from Scatchard analysis of the binding curves as indicated.

binding (24, 26). The apparent affinity of the bivalent rs-TNFRβ-hy3 fusion protein for TNFα and TNFβ was found to be significantly higher than the affinity of baculovirus- or CHO/dhfr$^-$-derived monovalent rsTNFRβ (Fig. 2). It is interesting to note that K_d values determined in the solid phase assay under high receptor density conditions (see "Experimental Procedures") were generally higher and did not show a marked difference in the apparent affinities between the fusion protein and rsTNFRβ (data not shown). It therefore appears that at maximum dense packing of the solid phase some interactions of receptor molecules leading to multiple valency and/or steric constrains cannot be excluded.

Stoichiometry of rsTNFRβ-TNFα and rsTNFRβ-TNFβ Complexes—rsTNFRβ purified from CHO/dhfr$^-$ cell culture medium was incubated with TNFα or TNFβ at different receptor to ligand molar ratios and fractionated according to size by gel filtration chromatography. The chromatographic conditions chosen allowed to separate receptor-ligand complexes from free receptor and free ligand. As shown in Fig. 3, at an approximate 1:1 molar ratio neither free receptor nor free TNFα or TNFβ could be detected in the elution profiles indicating that under these conditions complete complex formation had occurred. Amino acid composition analysis of the separated complexes evaluated by a recently described computer program (53) confirmed the 1:1 stoichiometry (not

shown). When the amount of TNFα added was gradually increased, a transition of the rsTNFRβ·TNFα complex toward a slightly lower molecular mass was observed in the elution profile (Fig. 3, *left panel*). In contrast, adding increasing amounts of TNFβ did not affect the elution behavior of the rsTNFRβ·TNFβ complex (Fig. 3, *right panel*).

To obtain a more accurate molecular mass estimate of rsTNFRβ and its complexes with TNFα and TNFβ, quasielastic light scattering and analytical ultracentrifugation studies were performed. The results are summarized in Table I. For rsTNFRβ a monomeric structure with a molecular mass of 25 kDa was found by sedimentation equilibrium analysis. The theoretical molecular mass for rsTNFRβ in its unglycosylated form is 20,467. Analysis of rsTNFRβ complexed to TNFα or TNFβ under conditions of complete complex formation (see below) yielded for both complexes a molecular mass of about 50 kDa. If a stoichiometry of three rsTNFRβ molecules bound to one 49-kDa TNFα or 57-kDa TNFβ trimer (9) is assumed, theoretical molecular masses of 124 and 132 kDa, respectively, are calculated which are in approximate agreement with the observed values. Sedimentation velocity analysis combined with quasielastic light scattering data confirmed the molecular masses observed in the equilibrium runs and were, in addition, indicative for a rather extended, *i.e.* rod-like structure of rsTNFRβ and its TNFα and TNFβ complexes.

Inhibition of TNFα and TNFβ Binding by rsTNFRβ and rsTNFRβ-hγ3—rsTNFRβ and rsTNFRβ-hγ3 were tested for their ability to competitively inhibit binding of TNFα and TNFβ to native TNFα and TNFβ purified from HL60 cells. In this assay native highly purified receptors were spotted onto nitrocellulose membranes and incubated with ^{125}I-TNFα or ^{125}I-TNFβ in the presence of different concentrations of rsTNFRβ or rsTNFRβ-hγ3. As shown in Fig. 4, *A* and *C*, binding of ^{125}I-TNFα to both TNF receptors was blocked by rsTNFRβ and rsTNFRβ-hγ3 in a concentration-dependent manner. It is interesting to note that a roughly equimolar concentration of the fusion protein was sufficient to prevent TNFα binding almost completely. rsTNFRβ was about 10–100 × less potent in inhibiting the binding. The binding of ^{125}I-TNFβ was also inhibited (Fig. 4, *B* and *D*), but higher concentrations of rsTNFRβ and rsTNFRβ-hγ3 were needed to achieve inhibitory effects comparable to TNFα. The 10–15% residual binding seen with iodinated TNFβ at high soluble receptor concentrations is due to nonspecific binding of radioactivity to the nitrocellulose filter.

The inhibition of TNF cytotoxicity by rsTNFRβ and rsTNFRβ-hγ3 was tested in a cellular cytotoxicity assay using the 2A3 subclone of the murine fibrosarcoma cell line WEHI164 (51). As expected from the binding studies, rsTNFRβ-hγ3 very efficiently inhibited TNF activity; at a concentration of 0.1 pmol/ml, *i.e.* equimolar to the TNFα concentration used in the assay, rsTNFRβ-hγ3 prevented TNFα-induced cytolysis very efficiently (Fig. 5*A*). rsTNFRβ also had inhibitory activity but a concentration about 100-fold in excess of TNFα was needed for complete inhibition. TNFβ-induced cytotoxicity was also inhibited by the fusion protein, albeit not at equimolar concentrations. The protective effects of rsTNFRβ in these cytotoxicity assays were only evident at rather high concentrations (Fig. 5*B*).

TNFα-induced Agglutination of rsTNFRβ-hγ3-coated Latex Beads—In view of the trimeric structure of TNFα and TNFβ each capable of binding three recombinant soluble receptor molecules, it is very likely that these cytokines aggregate TNF receptors on the cell surface into microclusters which may be a necessary step in signal transduction. To mimick cell sur-

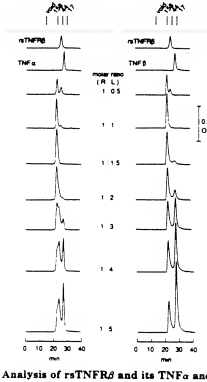

FIG. 3. **Analysis of rsTNFRβ and its TNFα and TNFβ complexes by gel filtration chromatography.** 1 nmol of rsTNFRβ purified from CHO/dhfr$^-$ cells was mixed with 0.5, 1, 1.5, 2, 3, 4, and 5 nmol of TNFα or TNFβ in 0.1 ml of PBS. (The amount of TNFα and TNFβ was calculated for the 17-kDa monomeric unit.) The mixtures with the various receptor:ligand (*R*:*L*) molar ratios were fractionated on a Superose 12 column (Pharmacia) in PBS. *Numbers* on *top* indicate the positions of molecular weight marker proteins (Bio-Rad). *Left panel*, TNFα complexes; *right panel*, TNFβ complexes.

TABLE I

Molecular mass determination of rsTNFRβ and its complexes with TNFα and TNFβ

Molecular masses were determined in the analytical ultracentrifuge as described under "Experimental Procedures." in the sedimentation velocity analyses the molecular masses were calculated according to the Svedberg equation using diffusion coefficients D determined in quasielatic light scattering measurements.

	Molecular mass (kDa)		
	Sedimentation equilibrium	Sedimentation velocity[a]	Putative stoichiometry
rsTNFRβ	25	20; 32	Monomer
rsTNFRβ·TNFα complex	140	115; 156	[TNFRβ] [TNFα]
rsTNFRβ·TNFβ complex	140	102; 139	[TNFRβ] [TNFβ]

[a] The 3rd and 0 moments of D were used in the calculation yielding molecular masses for a roughly spherical (listed first) and an extended (listed second) structure, respectively.

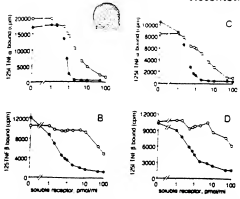

FIG. 4. **Binding of ^{125}I-TNFα and ^{125}I-TNFβ to native TNFRβ and TNFRα: inhibition by rsTNFRβ and rsTNFRβ-hy3.** Binding inhibition to native full-length TNFRβ and TNFRα purified from HL60 cells was measured in a dot blot assay as described under "Experimental Procedures." The concentration of radiolabeled ligand in the assay was 1 pmol/ml. *Open circles*, ligand binding in the presence of increasing concentrations of rsTNFRβ; *closed circles*, ligand binding in the presence of increasing concentrations of rsTNFRβ-hy3. (The concentration of the rsTNFRβ-hy3 homodimer was calculated for the 66-kDa monomer unit). *A*, ^{125}I-TNFα binding to TNFRβ; *B*, ^{125}I-TNFβ binding to TNFRβ; *C*, ^{125}I-TNFα binding to TNFRα; *D*, ^{125}I-TNFβ binding to TNFRα.

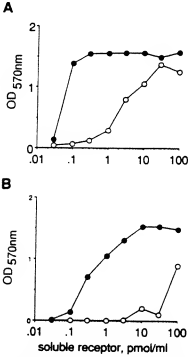

FIG. 5. **Inhibition of TNFα- and TNFβ-induced cytotoxicity in WEHI164 cells.** WEHI164 cells were cultured in the presence of 0.1 pmol/ml TNFα (*A*) or TNFβ (*B*) and different concentrations of rsTNFRβ (*open circles*) and rsTNFRβ-hy3 (*closed circles*). Cell viability was analyzed after 48 h at 37 °C.

face-bound TNF receptors, Latex beads were coated with rsTNFRβ-hy3 fusion protein and subsequently exposed to different concentrations of TNFα. TNFα induced an oligomerization of rsTNFRβ-hy3 as visualized by agglutination of the Latex beads (Fig. 6). A similar effect was seen with TNFβ, but agglutination was much less pronounced (results not shown).

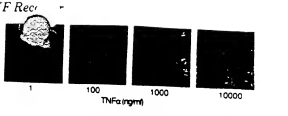

FIG. 6. **Agglutination of rsTNFRβ-hy3-coated Latex bead** Latex beads (0.48 μm diameter) were coated with rsTNFRβ-hy3 ar incubated at 1 mg/ml with different concentrations TNFα as ind cated. Agglutination of the beads was visualized in a light microscop at × 400 magnification.

DISCUSSION

In this study TNF binding and inhibiting properties of the extracellular region of the human TNFRβ were analyzed. The recombinant soluble receptors (rsTNFRβ and rsTNFRβ-hy fusion protein) expressed in different eukaryotic expressio systems displayed high affinity binding to human TNF similar to that of native cell surface-bound 55-kDa TNFR. In contrast, the binding affinity of rsTNFRβ for TNFβ we significantly decreased when compared with the native ce surface receptor. A similar observation, i.e. impaired neutra ization of TNFβ *versus* TNFα, has also been made with a sc called TNF binding protein, which is a naturally occurrin soluble receptor derived from TNFRβ (33, 36, 39). It therefor appears that with respect to ligand binding properties, rs TNFRβ closely ressembles the natural TNF inhibitor. Th apparent lower affinity of rsTNFRβ (and also of the deter gent-solubilized holoreceptor (9)) for TNFβ might reflect microenvironment of the ligand binding site which is slightl different from that of the cell surface-bound full-length TN receptor. It is noteworthy that with respect to monovalen rsTNFRβ the rsTNFRβ-hy3 fusion protein binds both TNF and TNFβ with a severalfold higher affinity when measure under appropriate assay conditions. This increase in affinit most probably reflects a higher avidity of the rsTNFRβ-hy construct due to its bivalency. Comparison of rsTNFRβ an the fusion protein to compete with native full-length TN receptors for TNF binding and to protect WEHI 164 cell from TNF-induced cytotoxicity indeed confirmed the ex pected higher activity of the fusion protein.

The results from the ultracentrifugation analyses indicat that rsTNFRβ is monomeric in solution. The complexes c rsTNFRβ with TNFα or TNFβ both had a molecular mass c about 140 kDa which favors a stoichiometry of three rsTNFR monomers bound to one TNFα or TNFβ trimer. It has bee proposed that the receptor binding site on the TNFα trime is located at the boundary of two monomeric units near th base of the bell-shaped structure thus implying three potenti receptor binding sites (7, 54). Such a model is fully compatibl with the size of receptor-ligand complexes as determined i the present study. It is interesting to note that an intermediat lower molecular weight form of the rsTNFRβ·TNFα comple can be partially resolved by gel filtration when a slight exces of TNFα over rsTNFRβ is present. Most likely, this inter mediate form represents TNFα trimers complexed to onl one or two rsTNFRβ molecules. Such intermediate forms ar not seen with rsTNFRβ·TNFβ complexes. Whether thes distinct binding characteristics of TNFα and TNFβ are als true for cell surface-bound receptors remains to be elucidate

The results of sedimentation velocity and quasielastic ligh scattering measurements indicate that rsTNFRβ and it TNFα and TNFβ complexes have a rather extended, i.e. roc like structure. This conclusion is supported by the relativ large apparent molecular masses of 62, 170, and 150 kDa fo rsTNFRβ, rsTNFRβ·TNFα and rsTNFRβ·TNFβ complexe respectively, determined by gel filtration chromatography similar relatively large apparent molecular mass (50 kDa) ha been found for the natural soluble TNFRβ on sizing columr (42).

Soluble fragments of both TNFRβ and TNFRα are found *in vivo*. They are present in relatively high concentrations in normal human serum and urine but can be drastically increased in certain disease states.[2] The cellular source and the mechanism of receptor shedding remain unclear. It has been speculated that soluble TNF receptor fragments might participate in the control of TNFα and/or TNFβ toxicity by neutralization and rapid clearance of systemic TNFα and TNFβ (33, 36, 37, 39, 42). However, the fact that at least a 10-fold excess of the soluble receptor with respect to TNFα (and more than a 100-fold excess with respect to TNFβ) is needed to obtain a significant neutralization demonstrates that the neutralizing capacity of serum is restricted. The rsTNFRβ-hγ3 construct as described in this study, therefore, is a promising TNF antagonizing agent for neutralization of systemic TNF toxicity in certain disease states.

Acknowledgment—We wish to thank Dr. M. Steinmetz for encouragement and support throughout this work, Drs. H. J. Schoenfeld, W. Hunziker, and E. Hochuli for providing TNFα and TNFβ, Dr. J. R. Frey for the WEHI164/2A3 clone, and Drs. K. Karjalainen, and A. Traunecker for the pCD4-hγ3-4 plasmid. The excellent technical assistance of H. P. Kurt, A. Hayes, U. Roethlisberger, and B. Syllwaschy is also gratefully acknowledged.

REFERENCES

1. Aggarwal, B. B., Kohr, W. J., Hass, P. E., Moffat, B., Spencer, S. A., Henzel, W. J., Bringman, T. S., Nedwin, G. E., Goeddel, D. V., and Harkins, R. N. (1985) *J. Biol. Chem.* **260**, 2345–2354
2. Gray, P. W., Aggarwal, B. B., Benton, C. V., Bringman, T. S., Henzel, W. J., Jarrett, J. A., Leung, D. W., Moffat, B., Ng, P., Svedersky, L. P., Palladino, M. A., and Nedwin, G. E. (1984) *Nature* **312**, 721–724
3. Pennica, D., Nedwin, G. E., Hayflick, J. S., Seeburg, P. H., Derynck, R., Palladino, M. A., Kohr, W. J., Aggarwal, B. B., and Goeddel, D. V. (1984) *Nature* **312**, 724–729
4. Nedospasov, S. A. (1986) *Nucleic Acids Res.* **14**, 7713–7725
5. Ware, C. F., and Green, L. M. (1987) *Lymphokines* **14**, 307–334
6. Devlin, J. J., Klostergaard, J., Orr, S. L., Yamamoto, R. S., Masunaka, I. K., Plunkett, J. M., and Granger, G. A. (1984) *Lymphokines* **9**, 313–336
7. Eck, M. J., and Sprang, S. R. (1989) *J. Biol. Chem.* **264**, 17595–17605
8. Jones, E. Y., Stuart, D. I., and Walker, N. P. C. (1989) *Nature* **338**, 225–228
9. Schoenfeld, H. J., Poeschl, B., Frey, H. R., Loetscher, H., Hunziker, W., Lustig, A., and Zulauf, M. (1991) *J. Biol. Chem.* **266**, 3863–3869
10. Vilček, J., Palombella, V. J., Henriksen-DeStefano, D., Swenson, C., Feinman, R., Hirai, M., and Tsujimoto, M. (1986) *J. Exp. Med.* **163**, 632–643
11. Sugarman, B. J., Aggarwal, B. B., Hass, P. E., Figari, I. S., Palladino, M. A., and Shepard, M. H. (1985) *Science* **230**, 943–945
12. Takeda, K., Iwamoto, S., Sugimoto, H., Takuma, T., Kawatani, N., Noda, M., Masaki, A., Morise, H., Arimura, H., and Konno, K. (1986) *Nature* **323**, 338–340
13. Collins, T., Lapierre, L. A., Fiers, W., Strominger, J. L., and Pober, J. S. (1986) *Proc. Natl. Acad. Sci. U. S. A.* **83**, 446–450
14. Johnson, D. R., and Pober, J. S. (1990) *Proc. Natl. Acad. Sci. U. S. A.* **87**, 5183–5187
15. Gamble, J. R., Harlan, J. M., Klebanoff, S. J., and Vadas, M. A. (1985) *Proc. Natl. Acad. Sci. U. S. A.* **82**, 8667–8671
16. Carswell, A. E., Old, L. J., Kassel, R. L., Green, S., Fiore, N., and Williamson, B. (1975) *Proc. Natl. Acad. Sci. U. S. A.* **72**, 3666–3670
17. Old, L. J. (1985) *Science* **230**, 630–632
18. Beutler, B., and Cerami, A. (1987) *N. Engl. J. Med.* **316**, 379–385
19. Talmadge, ... Phillips, H., Schneider, M., Rowe, T., Pennington, R., Bowers, ... and Lenz, B. (1988) *Cancer Res.* **48**, 544–550
20. Tracey, K. ... Lassara, H., and Cerami, A. (1989) *Lancet* **1**, 1122–1125
21. Beutler, B., ... Milsark, I. W., and Cerami, A. C. (1985) *Science* **229**, 869–87
22. Michie, H. R., Manogue, K. R., Spriggs, D. R., Revhaug, A., O'Dwyer, S., Dinarello, C. A., Cerami, A., Wolff, S. M., and Wilmore, D. W. (1988) *N. Engl. J. Med.* **318**, 1481–1486
23. Rothstein, J. L., and Schreiber, H. (1988) *Proc. Natl. Acad. Sci. U. S. A.* **85**, 607–611
24. Hohmann, H.-P., Remy, R., Brockhaus, M., and van Loon, A. P. G. M. (1989) *J. Biol. Chem.* **264**, 14927–14934
25. Brockhaus, M., Schoenfeld, H.-J., Schlaeger, H.-J., Hunziker, W., Lesslauer, W., and Loetscher, H. (1990) *Proc. Natl. Acad. Sci. U. S. A.* **87**, 3127–3131
26. Loetscher, H., Schlaeger, E. J., Lahm, H.-W., Pan, Y.-C. E., Lesslauer, W., and Brockhaus, M. (1990) *J. Biol. Chem.* **265**, 20131–20138
27. Loetscher, H., Pan, Y.-C. E., Lahm, H.-W., Gentz, R., Brockhaus, M., Tabuchi, H., and Lesslauer, W. (1990) *Cell* **61**, 351–359
28. Dembic, Z., Loetscher, H., Gubler, U., Pan, Y. C. E., Lahm, H. W., Gentz, R., Brockhaus, M., and Lesslauer, W. (1990) *Cytokine* **2**, 231–237
29. Heller, R. A., Song, K., Onasch, M. A., Fischer, W. H., Chang, D., and Ringold, G. M. (1990) *Proc. Natl. Acad. Sci. U. S. A.* **87**, 6151–6155
30. Smith, C. A., Davis, T., Anderson, D., Solam, L., Beckmann, M. P., Jerzy, R., Dower, S. K., Cosman, D., and Goodwin, R. G. (1990) *Science* **248**, 1019–1023
31. Schall, T. J., Lewis, M., Koller, K. J., Lee, A., Rice, G. C., Wong, G. H., Gatanaga, T., Granger, G. A., Lentz, R., Raab, H., Kohr, W. J., and Goeddel, D. V. (1990) *Cell* **61**, 361–370
32. Nophar, Y., Kemper, O., Brakebusch, C., Engelmann, H., Zwang, R., Aderka, D., Holtmann, H., and Wallach, D. (1990) *EMBO J.* **9**, 3269–3278
33. Kohno, T., Brewer, M. T., Baker, S. L., Schwartz, P. E., King, M. W., Hale, K. K., Squires, C. H., Thompson, R. C., and Vannice, J. L. (1990) *Proc. Natl. Acad. Sci. U. S. A.* **87**, 8331–8335
34. Gray, P. W., Barrett, K., Chantry, D., Turner, M., and Feldmann, M. (1990) *Proc. Natl. Acad. Sci. U. S. A.* **87**, 7380–7384
35. Loetscher, H., Brockhaus, M., Dembic, Z., Gentz, R., Gubler, U., Hohmann, H. P., Lahm, H. W., van Loon, A. P. G. M., Pan, Y. C. E., Schlaeger, E. J., Steinmetz, M., Tabuchi, H., and Lesslauer, W. (1991) in *Oxford Surveys on Eukaryotic Genes* (Maclean, N., ed) Oxford University Press, Oxford, in press
36. Engelmann, H., Aderka, D., Rubinstein, M., Rotman, D., and Wallach, D. (1989) *J. Biol. Chem.* **264**, 11974–11980
37. Engelmann, H., Novick, D., and Wallach, D. (1990) *J. Biol. Chem.* **265**, 1531–1536
38. Olsson, I., Lantz, M., Nilsson, E., Peetre, C., Thysell, H., Grubb, A., and Adolf, G. (1989) *Eur. J. Haematol.* **42**, 270–275
39. Seckinger, P., Isaaz, S., and Dayer, J.-M. (1989) *J. Biol. Chem.* **264**, 11966–11973
40. Gatanaga, T., Hwang, C., Kohr, W., Cappuccini, F., Lucci, J. A., Jeffes, E. W. B., Lentz, R., Tomich, J., Yamamoto, R. S., and Granger, G. A. (1990) *Proc. Natl. Acad. Sci. U. S. A.* **87**, 8781–8784
41. Peetre, C., Thysell, H., Grubb, A., and Olsson, I. (1988) *Eur. J. Haematol.* **41**, 414–419
42. Lantz, M., Gullberg, U., Nilsson, E., and Olsson, I. (1990) *J. Clin. Invest.* **86**, 1396–1402
43. Porteu, F., and Nathan, C. (1990) *J. Exp. Med.* **172**, 599–607
44. Traunecker, A., Schneider, J., Kiefer, H., and Karjalainen, K. (1989) *Nature* **339**, 68–70
45. Summers, M. D., and Smith, G. E. (1987) *Tex. Agric. Exp. Stn. Bull.* **1555**, 1–56
46. Schlaeger, E. J., and Schumpp, B. (1989) in *Advances in Animal Cell Biology and Technology for Bioprocessors* (Spiers, R. E., Griffiths, J. B., Stephenson, J., and Crooy, P. J., eds) pp. 386–396, Butterworth & Co. Ltd., Great Britain
47. Laemmli, U. K. (1970) *Nature* **227**, 680–685
48. Provencher, S. (1982) *Comput. Physics Comm.* **27**, 229–242
49. Durchschlag, H. (1989) *Colloid Polym. Sci.* **267**, 1139–1150
50. Chernyak, V. Y., Magretova, N. N., and Drachev, V. A. (1982) *Anal. Biochem.* **123**, 110–119
51. Peck, R., Brockhaus, M., and Frey, J. R. (1989) *Cell. Immunol.* **122**, 1–1
52. Hohmann, H.-P., Remy, R., Poschl, B., and van Loon, A. P. G. M. (1990) *J. Biol. Chem.* **265**, 15183–15188
53. Antoni, G., and Presentini, R. (1989) *Anal. Biochem.* **179**, 158–161
54. Tavernier, J., van Ostade, X., Hauquier, G., Prange, T., Lasters, I., de Maeyer, M., Lewit-Bentley, A., and Fourme, R. (1989) *FEBS Lett.* **257**, 315–318

[2] M. Brockhaus and H. Gallati, unpublished data.

40. Richmond, G. L. *Chem. Phys. Lett.* 110, [illegible]
41. Richmond, G. L., Rasing, H. M., Robinson, [illegible] & Shannon, V. L. *J. Opt. Soc. Am.* B4, 228-236 (1987).
42. Corn, R. M., Romagnoli, M., Levenson, M. D. & Philpott, M. R. *J. chem. Phys.* 81, 4127-4132 (1984).
43. Furtak, T. E., Miragliotta, J. & Korenowski, G. M. *Phys. Rev.* B 35, 2596-2572 (1987).
44. Richmond, G. L., Koos, D. A., Robinson, J. M. & Shannon, V. L. *Bull. Am. phys. Soc.* 33, 1648 (1988).
45. Shannon, V. L., Koos, D. A. & Richmond, G. L. *J. chem. Phys.* 87, 1440-1441 (1987); *Appl. Opt.* 26, 3579-3583 (1987).
46. Shannon, V. L., Koos, D. A. & Richmond, G. L. *J. phys. Chem.* 91, 5548-5555 (1987).
47. Shannon, V. L., Koos, D. A., Robinson, J. M. & Richmond, G. L. *Chem. Phys. Lett.* 142, 323-328 (1987).
48. Miragliotta, J. & Furtak, T. E. *Phys. Rev.* B 37, 1028-1030 (1988).
49. Rasing, Th., Kim, M. W., Shen, Y. R. & Grubb, S. *Phys. Rev. Lett.* 55, 2903-2906 (1985).
50. Berkovic, G., Rasing, Th. [illegible] Y. R. *J. chem. Phys.* 85, [illegible] (1986).
51. Bhattacharyya, K., Sitzmann, [illegible] & Eisenthal, K. B. *J. chem. Phys.* 87, 1442-1443 (1987).
52. Grubb, S. G., Kim, M. W., Rasing, Th. & Shen, Y. R. *Langmuir* 4, 452-454 (1988).
53. Freund, I. & Deutsch, M. *Opt. Lett.* 11, 94-96 (1986).
54. Heinz, T. F., Chen, C. K., Ricard, D. & Shen, Y. R. *Phys. Rev. Lett.* 48, 478-481 (1982).
55. Zhu, X. D., Suhr, H. & Shen, Y. R. *Phys. Rev.* B 35, 3047-3050 (1987).
56. Hunt, J. H., Guyot-Sionnest, P. & Shen, Y. R. *Chem. Phys. Lett.* 133, 189-192 (1987).
57. Guyot-Sionnest, P., Hunt, J. H. & Shen, Y. R. *Phys. Rev. Lett.* 59, 1597-1600 (1987).
58. Hunt, J. H., Guyot-Sionnest, P. & Shen, Y. R. in *Laser Spectroscopy VIII* (eds Persson, W. & Svanberg, S.) 253-266 (Springer, Berlin, 1987).
59. Guyot-Sionnest, P., Superfine, R. & Hunt, J. H. *Chem. Phys. Lett.* 144, 1-5 (1988).
60. Harris, A. L., Chidsey, C. E. D., Levinos, N. J. & Loiacono, D. N. *Chem. Phys. Lett.* 141, 350-356 (1987).
61. Superfine, R., Guyot-Sionnest, P., Hunt, J. H., Kao, C. T. & Shen, Y. R. *Surf. Sci.* 200, L445-L450 (1988).

ARTICLES

Designing CD4 immunoadhesins for AIDS therapy

Daniel J. Capon, Steven M. Chamow*, Joyce Mordenti†, Scot A. Marsters, Timothy Gregory*, Hiroaki Mitsuya‡, Randal A. Byrn§, Catherine Lucas||, Florian M. Wurm¶, Jerome E. Groopman§, Samuel Broder‡ & Douglas H. Smith

Departments of Molecular Biology, * Recovery Process Research and Development, † Pharmacological Sciences, || Medicinal and Analytical Chemistry, ¶ Cell Culture Research and Development, Genentech, Inc., 460 Point San Bruno Boulevard, South San Francisco, California, 94080, USA

‡ The Clinical Oncology Program, National Cancer Institute, National Institutes of Health, Bethesda, Maryland, 20892, USA

§ Division of Hematology-Oncology, Harvard Medical School, New England Deaconess Hospital, Boston, Massachusetts, 02215, USA

A newly-constructed antibody-like molecule containing the gp120-binding domain of the receptor for human immunodeficiency virus blocks HIV-1 infection of T cells and monocytes. Its long plasma half-life, other antibody-like properties, and potential to block all HIV isolates, make it a good candidate for therapeutic use.

DESPITE the exquisite ability of the immune system to distinguish between self and non-self, and to put forth an impressive diversity in its antigen-recognizing repertoire, it can still be outflanked by a rapidly changing pathogen. Human immunodeficiency virus type 1 (HIV-1) is an example of such a pathogen, and, as a result, its consequences are devastating. Every individual infected with the virus is expected to develop a serious or life-threatening illness[1]; no protective state has been shown to be generated in natural infections. It has not yet been possible to generate a protective response by immunizing chimpanzees with gp120, the HIV-1 envelope glycoprotein[2,3], or to confer passive immunity to chimpanzees using human IgG[4]. Even neutralizing antibodies made in experimental animals can block the infectivity of only a few HIV-1 isolates[3,5]. Thus, the prospects for eliciting protective immunity against HIV-1, or for using antibodies as therapeutic agents to control HIV-1 disease are bleak. Anti-retroviral chemotherapy using dideoxynucleosides such as AZT does help some patients, but the toxicity is such that new strategies are needed[6].

We have therefore attempted to block HIV-1 infectivity with soluble derivatives of CD4, the receptor for HIV-1, with the rationale that the CD4-binding domain of gp120 is the only part of gp120 that the virus cannot afford to change[7]. CD4 is a cell-surface glycoprotein found mostly on a subset of mature peripheral T cells that recognize antigens presented by class II MHC molecules[8,9]. Antibodies to CD4 block HIV-1 infection of T cells[10,11] and human cells not susceptible to HIV-1 infection become so after transfection with a CD4 cDNA[12]. Gp120 binds CD4 with high affinity ($K_D \sim 10^{-9}$M), suggesting that it is this interaction which is crucial to the entry of virus into cells[7,13]. Indeed, we[7] and others[14-18] have shown that soluble rCD4, lacking the transmembrane and cytoplasmic sequences of CD4, can block HIV-1 infectivity, syncytium formation, and cell killing by gp120 (ref. 19). rCD4 blocks the infectivity of diverse HIV-1 isolates (R.B., J.G., H.M. and S.B., unpublished results), and in theory should block all. At best, however, soluble rCD4 offers only a passive defence against the virus.

Active immunity requires a molecule such as an antibody, which can specifically recognize a foreign antigen or pathogen and mobilize a defence mechanism. Antibodies comprise two functionally independent parts, a rather variable domain (Fab), which binds antigen, and an essentially constant domain (Fc), providing the link to effector functions such as complement or phagocytic cells. It is almost certainly the lack of an antigen-binding domain which can neutralize all varieties of virus that hampers the development of humoural immunity to HIV-1. We reasoned that the characteristics of CD4 would make it ideal as the binding site of an antibody against HIV-1. Such an antibody would bind and block all HIV-1 isolates, and no mutation the virus could make, without losing its capacity to infect $CD4^+$ cells specifically, would evade it. We therefore set out to construct such an antibody by fusing CD4 sequences to antibody domains.

We had two major aims for our hybrid molecules; first, as pharmacokinetic studies in several species predict that the half-life of soluble CD4 will be short in humans (30-120 min, J.M., unpublished results) we wished to construct a molecule with a longer half-life; second, we wanted to incorporate functions such as Fc receptor binding, protein A binding, complement fixation and placental transfer, all of which reside in the Fc portion of IgG. The Fc portion of immunoglobulin has a long plasma half-life, like the whole molecule, whereas that of Fab is short, and we therefore expected to be able to fuse our short-lived CD4 molecule to Fc and generate a longer-lived CD4 analogue. Because CD4 is itself part of the immunoglobulin gene superfamily, we expected that it would probably fold in a way that is compatible with the folding of Fc. We have therefore produced a number of CD4-immunoglobulin hybrid molecules, using both the light and the heavy chains of immunoglobulin, and investigated their properties. We have named one

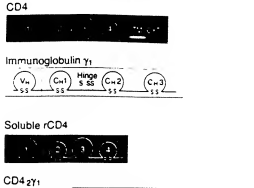

Fig. 1 Structure of cell surface CD4, human IgG1 (γ1), soluble rCD4, and CD4 immunoadhesins (2γ1 and 4γ1). The immunoglobulin-like domains of CD4 are numbered 1 to 4; TM and CYT refer to the transmembrane and cytoplasmic domains. Soluble rCD4 is truncated after proline 368 of the mature CD4 polypeptide. This results in a secreted, soluble polypeptide with an affinity for gp120 similar to that of cell surface CD4 (ref. 7). The vertical division within IgG1 indicates the junction of the variable (VH) and constant (CH1, hinge, CH2, and CH3) regions. Disulphide bonds formed within IgG1 domains and the immunoglobulin-like domains of CD4 are indicated by (S-S). The positions of cysteine residues that form intermolecular disulphide bridges connecting the IgG1 heavy-chain hinge to light and heavy chains are indicated by (S). CD4-derived and IgG1-derived domains of 2γ1 and 4γ1 are indicated by shaded and unshaded regions, respectively. The 2γ1 and 4γ1 immunoadhesins consist of residues 1 to 180 and residues 1 to 366 of the mature CD4 polypeptide, respectively, fused to the first residue (serine 114) of the human IgG1 heavy-chain constant region.

Methods. For the expression of CD4 immunoadhesins, the sequences of CD4 and human IgG1 were fused by oligonucleotide-directed deletional mutagenesis after their insertion into a mammalian expression vector used for soluble rCD4 expression[7]. A human IgG1 heavy-chain cDNA, obtained from a human spleen cDNA library using probes based on the published sequence[47], was inserted at a unique *Xba*I site found immediately 3′ of the CD4 coding region in the same reading orientation as CD4. Synthetic 48-mer oligodeoxynucleotides, complementary to the 24 nucleotides at the borders of the desired CD4 and IgG1 fusion sites, were used as primers in the mutagenesis reactions using the plasmid described above as the template[48].

particularly interesting class of these CD4-immunoglobulin hybrids 'immunoadhesins', because they contain part of an adhesive molecule[20] linked to the immunoglobulin Fc effector domain.

Synthesis of CD4 immunoadhesins

CD4 is an integral membrane protein with an extracellular region comprising four domains with homology to immunoglobulin variable domains[21,22] (Fig. 1). Soluble CD4 derivatives consisting of this extracellular region bind gp120 with the same affinity as cell-surface CD4 (ref. 7). CD4 variants containing only domains 1 and 2 also bind gp120[17,18], but the affinity of this interaction is not known. We constructed a series of hybrid molecules consisting of the first two or all four immunoglobulin-like domains of CD4 fused to the constant region of antibody heavy and light chains (Fig. 1).

We investigated the synthesis and secretion of these hybrids using transient expression in a human embryonic kidney-derived cell line. As shown in Fig. 2, immunoglobulin light and heavy chains are efficiently expressed in these cells, and light chain is efficiently secreted, but heavy chain is not unless a light chain is coexpressed. Thus the rules governing immunoglobulin chain secretion in these cells are the same as those for plasma or other lymphoid cells[23]. We first constructed hybrids that fused CD4 with the constant regions of murine κ- or γ1-chains. These hybrids contained either the first two or all four immunoglobulin-like domains of CD4, linked at a position chosen to mimic the spacing between disulphide-linked cysteines seen in immunoglobulins (Fig. 1). As expected, the CD4-κ hybrids were secreted well, whereas hybrids between CD4 and mouse γ1-chain were expressed but not secreted unless a κ-chain or a CD4-κ hybrid was present.

A different and unexpected picture emerged when analogous CD4-heavy-chain hybrids were constructed using the constant region of human IgG1 heavy chain instead of mouse heavy chain. Such hybrids, containing either the first two or all four immunoglobulin-like domains of CD4 (named 2γ1 and 4γ1 respectively), were secreted in the absence of wild-type or hybrid light chains (Fig. 2*a*). Both 2γ1 and 4γ1 could be directly immunoprecipitated using *Staphylococcus aureus* protein A, which binds the Fc portion of IgG1, indicating that the protein A-binding sites of these constructs are fully functional. Indeed, both molecules can be purified to near homogeneity on protein A columns (Fig. 2*b*).

Structure of CD4 immunoadhesins

We examined the subunit structure of these immunoadhesin molecules using SDS-polyacrylamide gels (Fig. 2*b*). Without any reducing agent, the apparent relative molecular mass (M_r) of each construct doubled, demonstrating that both immunoadhesins are disulphide-linked dimers. The hinge region of each immunoadhesin contains three cysteine residues, one normally involved in disulphide bonding to light chain, the other two in the intermolecular disulphide bonds between the two heavy chains in IgG. As the molecules are dimers at least one, and perhaps all three, of these cysteine residues are involved in intermolecular disulphide bonds. We examined the capacity of 2γ1 and 4γ1 to form disulphide links with light chains. When an immunoadhesin construct was cotransfected with a light chain, the light chain produced could be precipitated by protein A. Mutagenic substitution of the first hinge-region cysteine with alanine abolished light-chain bonding, but did not affect dimerization (data not shown), indicating that this cysteine bonds the light chain in these hybrids, as in normal IgG. Thus the disulphide bond structure of these immunoadhesins seems to be analogous to that of immunoglobulins.

gp120 binding

To determine whether our immunoadhesins retain the ability to bind gp120 with high affinity, and whether the first two immunoglobulin-like domains are sufficient, we carried out saturation binding analyses with radioiodinated gp120. Binding is saturable, showing a simple mass action curve (Fig. 3*a*). The dissociation constant (K_d) for the interaction of each immunoadhesin with gp120, calculated by Scatchard analysis (Fig. 3*a*, inset), was indistinguishable from that of soluble rCD4 ($\sim 10^{-9}$ M) (Table 1). Thus, the N-terminal 170 amino acids of CD4 are sufficient for high-affinity binding. As these immunoadhesins are homodimeric, they should each have two gp120-binding sites. We examined this possibility by coating plastic microtitre wells with gp120, then adding soluble CD4 or immunoadhesins. Both immunoadhesins could bind added labelled gp120, whereas soluble rCD4, with only one gp120 binding site, could not (J. Porter and S. C., unpublished results). To confirm the bivalent nature of 2γ1 and 4γ1, we examined their ability to agglutinate sheep red blood cells coated with gp120. Again, both CD4-immunoadhesins, but not soluble rCD4, agglutinated the cells, showing that binding to gp120 molecules on different cells is not sterically hindered

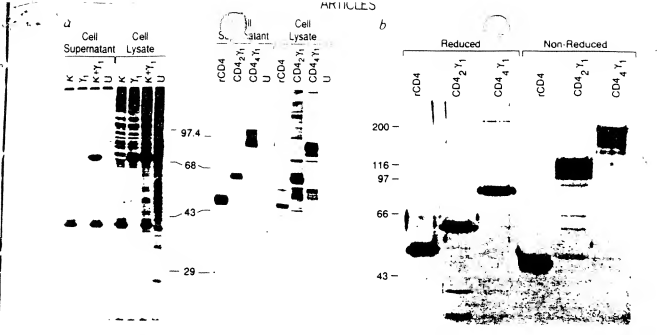

Fig. 2 Expression, secretion and subunit structure of CD4 immunoadhesins and soluble rCD4. *a*, Expression and secretion of mouse immunoglobulins, soluble rCD4 and CD4 immunoadhesins expressed in mammalian cells. Cells were transfected with vectors directing the expression of murine κ-light chain (lanes κ) or γ1-heavy chain (lanes γ1) individually or together (lanes κ + γ1), vectors encoding soluble rCD4 (lanes rCD4), and the CD4 immunoadhesins 2γ1 (lanes $CD4_2\gamma_1$) or 4γ1 (lanes $CD4_4\gamma_1$). After metabolic labelling with [^{35}S]methionine, cell supernatants and cell lysates were analysed by immunoprecipitation. Lanes U, untransfected cells. *b*, Subunit structure of secreted CD4 immunoadhesins and soluble rCD4. Soluble rCD4, 2γ1 and 4γ1 were purified from culture supernatants of transfected cells and analysed by electrophoresis on a 7.5% SDS-polyacrylamide gel. Samples were prepared in buffer with 10 mM dithiothreitol (DTT) (reducing conditions) or without DTT (non-reducing conditions). The positions of relative molecular mass standards are indicated (in thousands). Both immunoadhesins behaved as disulphide-linked dimers; in contrast, soluble rCD4 which is monomeric, displayed only a minor change in mobility upon reduction of its intra-molecular disulphide bonds.

Methods. *a*, Cells were transfected by a modification of the calcium phosphate procedure, labelled with [^{35}S]methionine, and cell lysates prepared as described[7]. Immunoprecipitation analysis was carried out as previously described[7], with the exception that no preadsorbtion with Pansorbin (Calbiochem) was done, and the precipitating antibodies used were 2 μl of rabbit anti-mouse IgG serum (Cappel) for mouse IgG heavy and light chains, 0.25 μg of OKT4A (Ortho) for soluble rCD4, and no added antibody (Pansorbin only) for the CD4 immunoadhesins. Immunoprecipitated proteins were resolved on 10% SDS-PAGE gels, and visualized by autoradiography. *b*, CD4 immunoadhesins were purified from transfected cell supernatants by protein A affinity chromatography followed by ammonium sulphate precipitation. Purified proteins were subjected to SDS-PAGE under both reducing and non-reducing conditions and visualized by silver staining.

In vivo plasma half-life

We examined whether the immunoadhesins share the long *in vivo* half-life of antibodies. Studies of rCD4 in rabbits provide clearance data that extrapolate well to other species, including humans (J.M., unpublished results). The change in plasma concentration with time for each of the three CD4 analogues in rabbits is shown in Fig. 4. Analysis of these data reveals that soluble rCD4 has a terminal half-life in rabbits of ~15 min, whereas 4γ1 and 2γ1 have terminal half-lives of ~7 and 48 h, respectively (Table 1). Thus the half-life of 2γ1 in rabbits is nearly 200 times longer than that of rCD4 and comparable to that of human IgG in rabbits (4.7 days)[24]. The half-life of 2γ1 in humans is expected to be longer than that in rabbits, because of the decreased proportional blood flow to eliminating organs as species increase in size[25], and should be comparable with that of human IgG1 (21 days).

Our results confirm our initial hypothesis that, as in the case of immunoglobulin itself, one can increase the stability of a rapidly cleared molecule (Fab or rCD4) by fusing it to a long-lived molecule, Fc. The swift clearance of rCD4 is probably largely due to its size, M_r 55,000, which means it is just small enough to be cleared efficiently by renal filtration. One component in the increased half-lives of these molecules is therefore probably their larger size; but this cannot be the whole story as 4γ1, although larger than 2γ1, has a shorter half-life. Both 4γ1 and rCD4, but not 2γ1, contain two CD4-derived Asn-linked carbohydrate sites which are glycosylated in rCD4 (R. Harris and M. Spellman, unpublished results); these sugar moieties

Table 1 Properties of CD4 immunoadhesins and soluble rCD4

	Calculated M_r	Subunit structure	gp120 binding (nM)*	Blocks infectivity T cells	Blocks infectivity Mϕ	Plasma half-life in rabbits (hours)†	Fc binding (nM)*	Complement binding	Protein A binding
rCD4	41,000	monomer	2.3 ± 0.4	Yes	Yes	0.25 ± 0.01	—	No	No
4γ1	154,000	dimer	1.2 ± 0.1	Yes	Yes	6.7 ± 1.1	2.3 ± 0.7	No	Yes
2γ1	112,000	dimer	1.4 ± 0.1	Yes	Yes	48.0 ± 8.6	2.6 ± 0.3	No	Yes
IgG1	146,000	tetramer (H_2L_2)	—	—	—	113‡	3.2 ± 0.2	Yes	Yes

* Standard error of the mean was determined using the Inplot and Scatplot programs (see Fig. 3 legend). † Standard deviation indicated in hours.
‡ Determined in ref. 24 (IgG1 has a half-life of 21 days in humans).

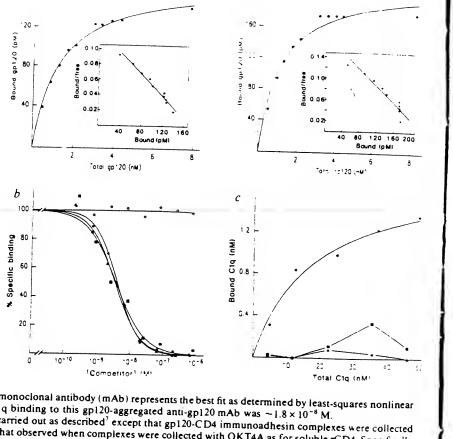

Fig. 3 Binding properties of CD4 immunoadhesins. *a*, Gp120 saturation binding analysis of CD4 immunoadhesins. Immunoadhesin proteins 4γ1 (left) or 2γ1 (right) in transfected cell supernatants were incubated with increasing concentrations of purified soluble rgp120 (ref. 50) radioiodinated with lactoperoxidase. The lines drawn for the binding curves and for the Scatchard plots of the data (shown in the insets) represent the best fit as determined by unweighted least-squares linear regression analysis. Dissociation constants calculated from these results and from binding studies of gp120 to soluble rCD4 performed in parallel are given in Table 1. *b*, Binding of CD4 immunoadhesins to $Fc\gamma$ receptors on U937 cells. Competition binding analysis was carried out by mixing 0.1 μg ml^{-1} of ^{125}I-labelled human IgG1 (Calbiochem) with increasing concentrations of purified human IgG1 (solid circle), 2γ1 (solid square), 4γ1 (solid triangle), or soluble rCD4 (open circle) proteins. Curves drawn represent the best fit as determined by unweighted least-squares nonlinear (IgG1, 2γ1 and 4γ1) or linear (rCD4) regression analysis. Dissociation constants calculated from these results are shown in Table 1. *c*, C1q saturation binding analysis of CD4 immunoadhesins. Purified anti-gp120 IgG2a mouse monoclonal antibody (solid circle), 2γ1 (solid square), or 4γ1 (solid triangle) proteins were aggregated by binding to gp120-coupled Sepharose, and incubated with increasing concentrations of purified human C1q (Calbiochem) radioiodinated with lactoperoxidase. The curve drawn for the anti-gp120 monoclonal antibody (mAb) represents the best fit as determined by least-squares nonlinear regression analysis; the dissociation constant for C1q binding to this gp120-aggregated anti-gp120 mAb was ~1.8×10^{-9} M.

Methods. *a*, Gp120 saturation binding analysis was carried out as described[7] except that gp120-CD4 immunoadhesin complexes were collected directly onto Pansorbin: binding was comparable to that observed when complexes were collected with OKT4A as for soluble rCD4. Specifically, bound ^{125}I-labelled gp120 was determined from the difference in binding in the presence or absence of a 1,000-fold excess of unlabelled rgp120 and is plotted against the total ^{125}I-labelled gp120 concentration. *b*, FcR binding analysis was done essentially as described[27] except that after centrifugation free IgG1 was removed by aspiration of the aqueous and oil layers. Mixtures of ^{125}I-labelled human IgG1 and IgG1, CD4 immunoadhesins or soluble rCD4 were incubated with U937 cells (2×10^6 cells per tube) for 60 min at 4 °C. Specific binding was calculated by subtracting residual nonspecific binding (<25% of specific binding) which could not be competed out by a 1,000-fold excess of unlabelled human IgG1. *c*, C1q binding analysis was done essentially as described[29], except that gp120 coupled to CNBr-activated Sepharose 6B (Pharmacia) was used as the solid support to aggregate CD4 immunoadhesins or the anti-gp120 mouse mAb. Proteins were adsorbed to gp120 coupled beads, incubated with varying concentrations of ^{125}I-labelled C1q, and bound and free C1q were then separated by centrifugation through 20% sucrose. Specific binding was determined from the difference in binding in the presence or absence of added antibody or immunoadhesin. All data analysis was carried out using the Inplot and Scatplot programs (R. Vandlen, Genentech). Scatplot was modified from the Ligand program (P. Munro, NIH).

may facilitate clearance by receptors in the liver. The charge of the molecule may also be important, as the CD4 portion of 4γ1 contributes a net excess of eleven positively charged amino acids on 4γ1, but only three on 2γ1. This may increase uptake of rCD4 and 4γ1 onto antionic surfaces, accelerating their clearance from the circulation.

Fc receptor and complement binding

Two major mechanisms for the elimination of pathogens are mediated by the Fc portion of specific antibodies. Fc activates the classical pathway of complement, ultimately resulting in lysis of the pathogen, whereas binding to cell Fc receptors can lead to ingestion of the pathogen by phagocytes or lysis by killer cells. The binding sites for Fc cell receptors and for the initiating factor of the classical complement pathway, C1q, are found in the constant region of heavy chain[26] (the CH2 domain for C1q[22] and the region linking the hinge to CH2 for Fc cell receptors[28]). We aimed to incorporate both of these functions into the immunoadhesins. We chose the IgG1 subtype to supply the Fc domain because IgG1 is the best compromise between Fc binding, C1q binding, and long half-life. We show below that the immunoadhesins bind FcR well, but do not bind C1q.

Three types of Fc cell receptors are known to be expressed on a variety of leukocytes. Of these FcR1, principally expressed on mononuclear phagocytes, is the only one which binds monomeric human IgG1 with high affinity[56]. We used competition binding analysis with FcR1 receptors on the U937 monocyte/macrophage cell line to characterize the Fc receptor binding of 2γ1 and 4γ1. Direct saturation binding analysis with human IgG1 gave a K_d of ~3×10^{-9} M. In competition binding analyses, the two CD4 immunoadhesins, but not rCD4, bound to Fc receptors on U937 cells to the same extent and with an affinity indistinguishable from human IgG1 (Fig. 3*b*, Table 1).

We examined the ability of the immunoadhesins to bind to the first component of the classical pathway of complement, C1q, by saturation binding analysis. Because binding of C1q increases with the aggregation state of the antibody, with an affinity of ~10^{-8} for monomers and ~10^{-9} for tetramers of IgG[26], we first aggregated the immunoadhesin using gp120 linked to Sepharose. As a positive control, we measured C1q binding to an anti-gp120 mouse IgG2a monoclonal antibody (which like human IgG1 binds C1q with high affinity[57]) aggregated by the same gp120-Sepharose. The affinity of the mouse antibody for C1q determined by Scatchard analysis was 1.8×10^{-9} M (Fig. 3*c*), comparable to that observed for other mouse IgG2a and for human IgG1 antibodies. In contrast, neither immunoadhesin bound C1q to any detectable extent (Fig. 3*c*).